Estimating the effect of operational loading conditions from ultrasonic guided wave measurements using an iterated Unscented Kalman Filter

André Luiz Dalmora[1,2,3], Alexandre Imperiale[1], Sébastien Imperiale[2,3], Philippe Moireau[2,3]

[1] Université Paris-Saclay, CEA, List, F-91120, Palaiseau, France
[2] Project-Team M3DISIM, Inria Saclay-Ile-de-France, Inria, 91128 Palaiseau, France
[3] LMS, École Polytechnique, CNRS, Institut Polytechnique de Paris, 91128 Palaiseau, France

10/05/2023 – GdR MecaWave 2023

- **Context:**
  - Modeling and Simulation for NDT, in particular SHM.
  - SHM: Environmental and Operational conditions (EOCs).
    Mechanical loading conditions *in situ*. Gorgin et al. 2020

- **Colloque GdR MecaWave 2021 (direct model):**
  Combining shell elements and transient spectral finite elements for guided wave propagation problems in prestressed thin structures.

- **Objective:**
  Propose an inverse strategy to reconstruct loading conditions using ultrasonic guided waves measurements.

  - Direct model: Linearized elastodynamic model solved using 3D Spectral Finite Elements. Dalmora et al. 2022
  - Inversion: Iterated Unscented Kalman Filtering.

Use case example

Test stand of 4-point bending tests at IMA Dresden GmbH within the project QuantSHM (funding code 100207022) which was funded by the federal state of Saxony via the Sächsische Aufbaubank. (Image provided by Fraunhofer IKTS, a partner in the GW4SHM project.)

- **The pipe is subjected to a force of 220kN which oscillates up to 2Hz.**
- **A weld with a defect is located between the transducer rings.**
- **The effect of prestresses significantly reduced the probability of detection of the defect.**

Input

Output

Mechanical loading causing deformation + Ultrasonic Source

Direct Model

Wavefield

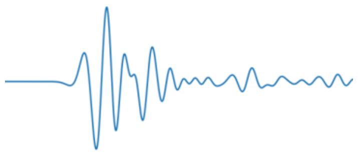

Measurements by sparse ultrasonic transducers

Inversion Algorithm

Estimation of the deformation

Outline

Input

Output

Mechanical loading
causing deformation
+ Ultrasonic Source

Direct Model

Wavefield

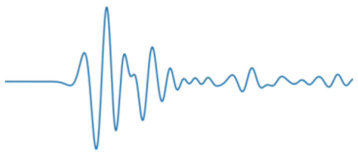

Measurements by sparse
ultrasonic transducers

Inversion Algorithm

Estimation of the
deformation

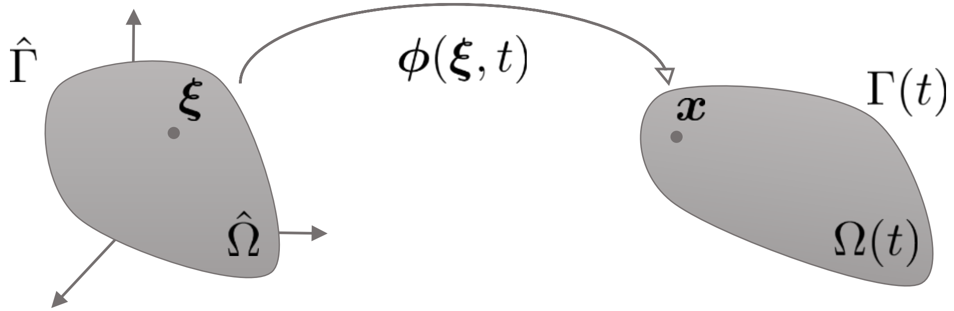

Starting from the nonlinear elastodynamics in its strong formulation

$$\begin{cases} \rho \dfrac{\partial^2 \boldsymbol{u}}{\partial t^2} - \boldsymbol{\nabla}_{\boldsymbol{x}} \cdot \boldsymbol{\sigma} = \rho \boldsymbol{f} & \text{on } \Omega(t), \\ \boldsymbol{\sigma} = \boldsymbol{G}(\boldsymbol{e}) & \text{(hyperelastic)}, \\ \boldsymbol{u} = 0 & \text{on } \Gamma^D, \end{cases} \quad \text{with} \quad \boldsymbol{F} = \boldsymbol{\nabla}_{\xi}\, \phi, \quad \boldsymbol{C} = \boldsymbol{F}^\intercal \boldsymbol{F}, \quad \boldsymbol{e}(\boldsymbol{u}) = \frac{1}{2}(\boldsymbol{C} - 1).$$

Method: Knowing that the associated forces differ in their natures, we decompose the problem in two sub-problems

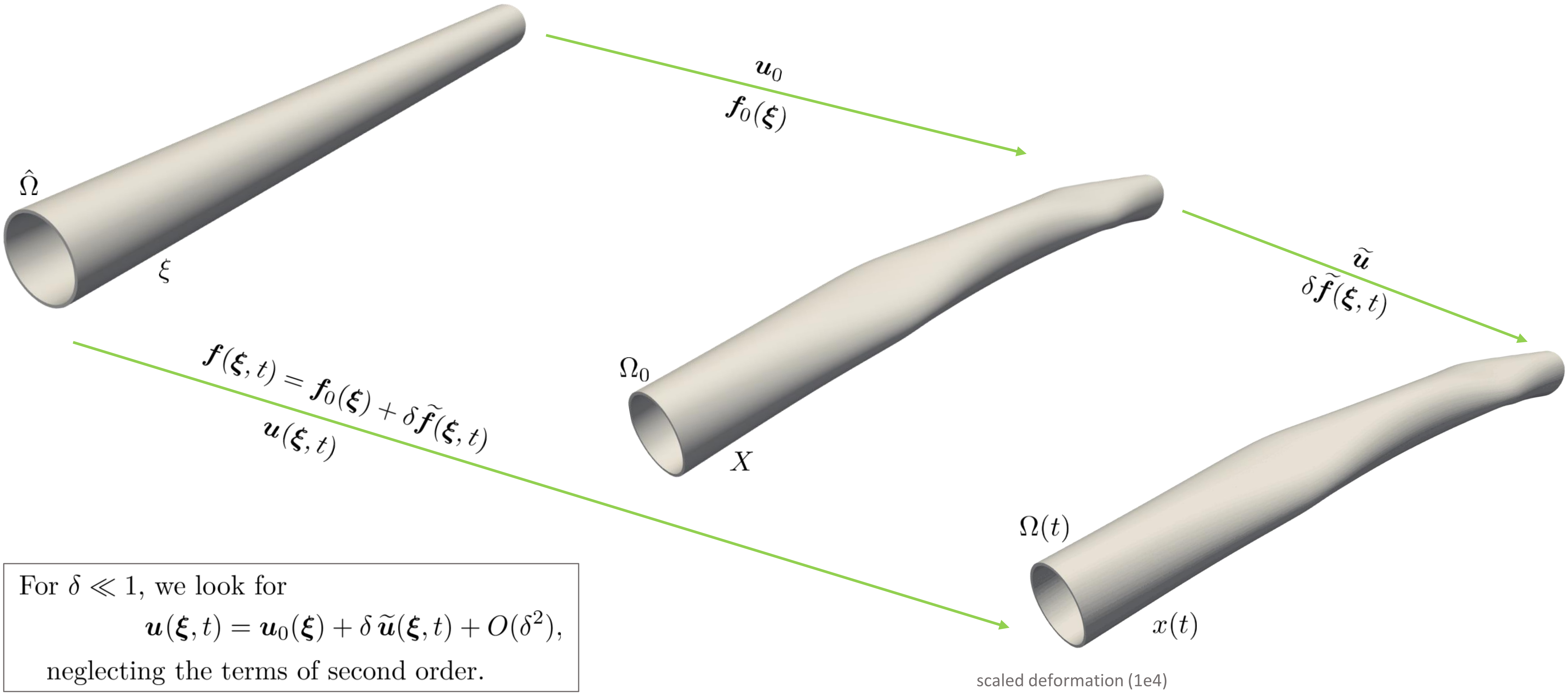

For $\delta \ll 1$, we look for

$$\boldsymbol{u}(\boldsymbol{\xi},t) = \boldsymbol{u}_0(\boldsymbol{\xi}) + \delta\,\widetilde{\boldsymbol{u}}(\boldsymbol{\xi},t) + O(\delta^2),$$

neglecting the terms of second order.

Weak formulation

$$\forall w \in \mathcal{V}(\hat{\Omega}),$$

$$\frac{\mathrm{d}^2}{\mathrm{d}t^2} m[u,w] + a(u)[w] = l[w]$$

$$\left| \begin{aligned} m[u,w] &= \int_{\hat{\Omega}} \hat{\rho}\, \boldsymbol{u} \cdot \boldsymbol{w} \mathrm{d}\hat{\Omega}, \\ a(u)[w] &= \int_{\hat{\Omega}} \boldsymbol{\Sigma}(\boldsymbol{e}) : \mathrm{D}_{\boldsymbol{u}} \boldsymbol{e}(\boldsymbol{u})[\boldsymbol{w}]\, \mathrm{d}\hat{\Omega}, \\ l[w] &= \int_{\hat{\Omega}} \hat{\rho} \boldsymbol{f} \cdot \boldsymbol{w}\, \mathrm{d}\hat{\Omega}. \end{aligned} \right.$$

+

Linearization

$$\boldsymbol{f}(\boldsymbol{\xi}, t) = \boldsymbol{f}_0(\boldsymbol{\xi}) + \delta \widetilde{\boldsymbol{f}}(\boldsymbol{\xi}, t)$$

$$\boldsymbol{u}(\boldsymbol{\xi}, t) = \boldsymbol{u}_0(\boldsymbol{\xi}) + \delta\, \widetilde{\boldsymbol{u}}(\boldsymbol{\xi}, t) + O(\delta^2)$$

+ separating terms in δ.

- **Structural deformation: Nonlinear and static.**

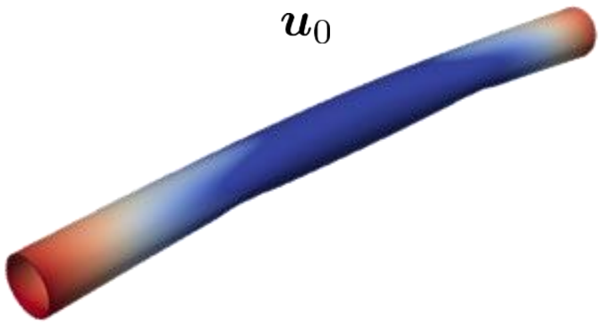

$$a(u_0)[w] = l_0(w)$$

- 3D Shell Finite Elements, avoiding numerical locking in thin structures.

Chapelle and Bathe 2011

- **MoReFEM** code (MΞDISIM - Inria team)

- **Wave propagation: Linearized and high frequency.**

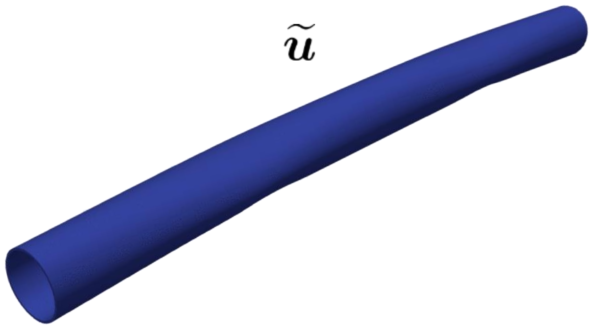

$$\frac{\mathrm{d}^2}{\mathrm{d}t^2} m[\widetilde{u}, w] + \mathrm{D}_u a(u_0)[\widetilde{u}, w] = \widetilde{l}[w]$$

- Time domain (Explicit Leap Frog).
- SFEM kernel **CIVA**(CEA)

Maday and Patera. 1989 ; Cohen 2002

Operators

$$a(u_0)[w] = \int_{\hat{\Omega}} \boldsymbol{\Sigma}(\boldsymbol{e}_0) : \mathrm{D}_{\boldsymbol{u}} \boldsymbol{e}(\boldsymbol{u}_0)[\boldsymbol{w}]\, \mathrm{d}\hat{\Omega}$$

$$l_0[w] = \int_{\hat{\Omega}} \hat{\rho} \boldsymbol{f}_0 \cdot \boldsymbol{w}\, \mathrm{d}\hat{\Omega}.$$

$$m[\widetilde{u}, w] = \int_{\hat{\Omega}} \hat{\rho}\, \widetilde{\boldsymbol{u}} \cdot \boldsymbol{w}\, \mathrm{d}\hat{\Omega},$$

$$\mathrm{D}_u a(u_0)[\widetilde{u}, w] = \int_{\hat{\Omega}} \mathrm{D}_{\boldsymbol{u}} \boldsymbol{e}(\boldsymbol{u}_0)[\widetilde{u}] : \mathrm{D}_{\boldsymbol{e}} \boldsymbol{\Sigma}(\boldsymbol{e}_0) : \mathrm{D}_{\boldsymbol{u}} \boldsymbol{e}(\boldsymbol{u}_0)[\boldsymbol{w}]\, \mathrm{d}\hat{\Omega} + \int_{\hat{\Omega}} \boldsymbol{\Sigma}(\boldsymbol{e}_0) : \mathrm{D}^2_u \boldsymbol{e}[\widetilde{\boldsymbol{u}}, \boldsymbol{w}]\, \mathrm{d}\hat{\Omega},$$

$$\widetilde{l}[w] = \int_{\hat{\Omega}} \hat{\rho} \widetilde{\boldsymbol{f}} \cdot \boldsymbol{w}\, \mathrm{d}\hat{\Omega}.$$

Remark on implementation $\forall w \in \mathcal{V}(\hat{\Omega}),\quad \frac{\mathrm{d}^2}{\mathrm{d}t^2} m[\tilde{u}, w] + \mathrm{D}_u a(u_0)[\tilde{u}, w] = \tilde{l}[w]$

Discretizing by conform FE we have $\frac{\mathrm{d}^2}{\mathrm{d}t^2}\mathbb{M}\vec{u} + \mathbb{K}'(u_0)\vec{u} = \vec{f}$

Using a leapfrog time scheme $\vec{u}^{n+1} = -\Delta t^2 \mathbb{M}^{-1}\mathbb{K}'(u_0)\vec{u}^n + \Delta t^2 \mathbb{M}^{-1}\vec{f} + 2\vec{u}^n - \vec{u}^{n-1},$

Lumped mass

Parallelized non-assembled operation

Important aspects:

- Solving for **arbitrary hyperelastic constitutive law, geometry and mechanical loading**.
- High efficiency due to lumped-mass and parallelization.
- Non-assembled stiffness: low memory usage and inexpensive “parameter” update.
- Stability: operator non-negativeness must be assured.
- Strategy **validated** with experimental data.

Why estimate the loading in the context of SHM?

Wave propagation

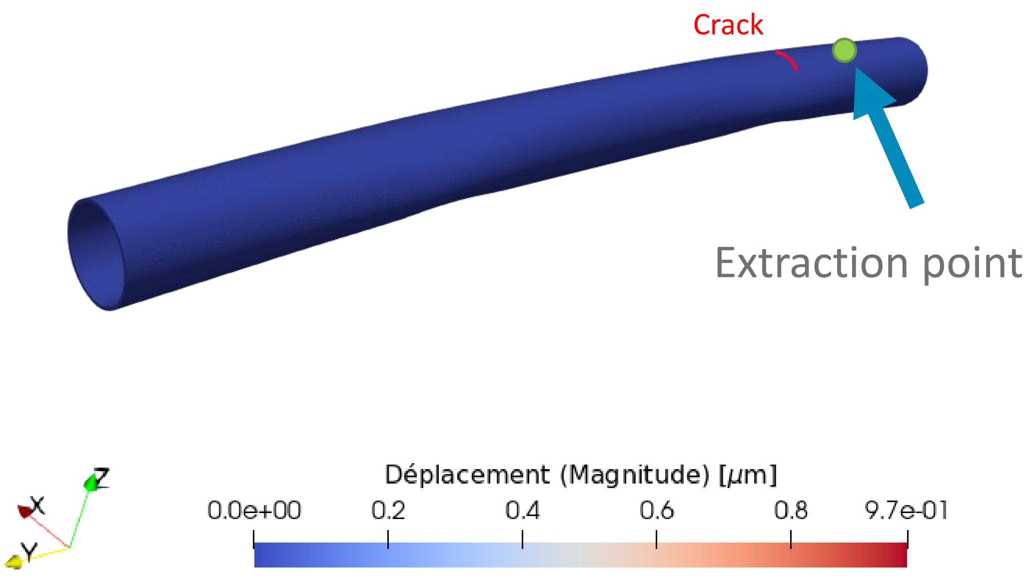

The effect of loading on wave propagation is evaluated numerically and compared with the effect of a defect. Considering the extracted simulated signals

- S: non deformed pipe (baseline; no defects).
- S_p: deformed pipe (without defect).
- S_d: pipe with defect (without deformation).

Effect of the defect vs prestresses

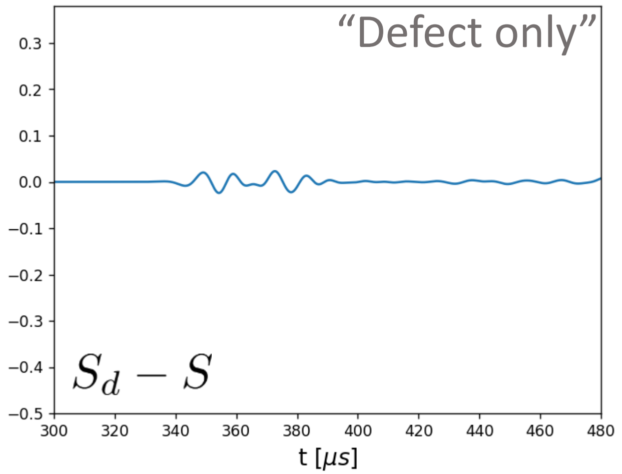

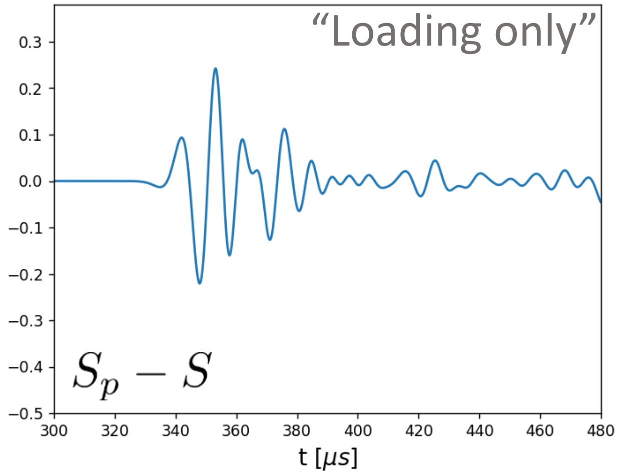

Outline

Input

Mechanical loading
causing deformation
+ Ultrasonic Source

Direct Model

Output

Wavefield

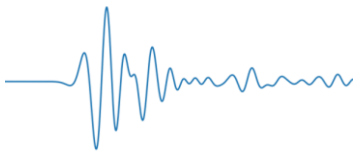

Measurements by sparse
ultrasonic transducers

Inversion Algorithm

Estimation of the
deformation

Loading condition reconstruction

Reconstructing loading deformation by means of limited ultrasonic measurements.

Direct model: $$\frac{\mathrm{d}^2}{\mathrm{d}t^2} m[\tilde{u}, w] + \mathrm{D}_u a(u_0)[\tilde{u}, w] = \tilde{l}(w)$$

Objective: reconstruct u_0 using limited information over $\tilde{u}$.

We interpret the inverse problem as minimizing a least-squares misfit between measurements and data generated from the model.

Functional:

number of measured signals

measurements

$$\mathcal{J}(u_0) = \min_{u_0} \frac{1}{2} \Big\{ \|u_0\|^2_{\mathbb{P}^{-1}_{u_0}} + \frac{1}{N_s} \sum_i^{N_s} \int_0^T \|y(t) - C_i(\tilde{u}|_{u_0}(t))\|^2_{\mathbb{S}} dt \Big\}.$$

Regularization norm

observation operator

wavefield generated for the deformation u_0

It represents a nonlinear minimization problem.

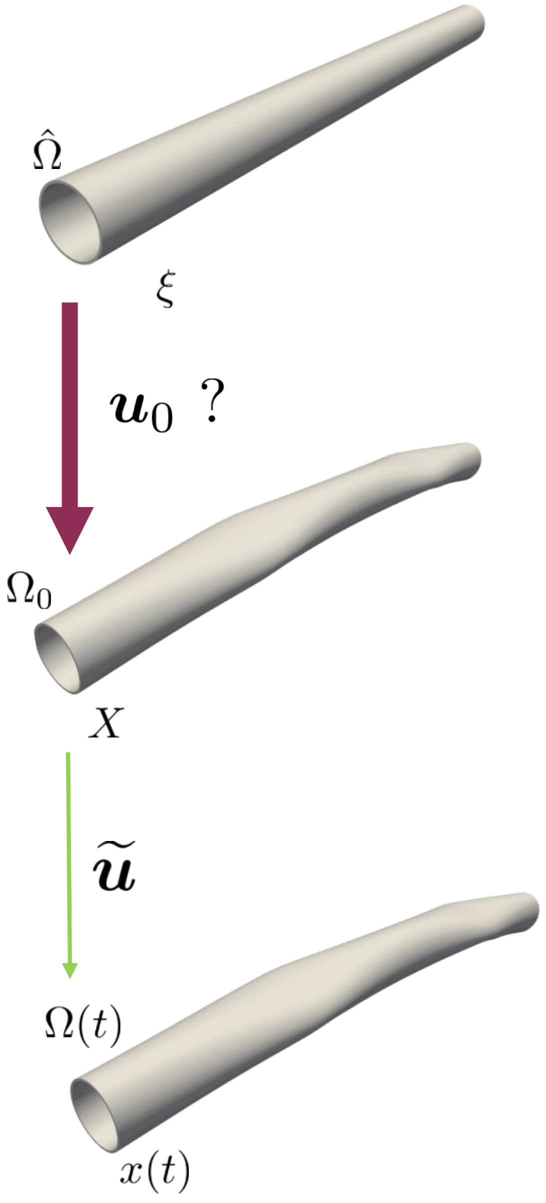

Direct model: $$\frac{\mathrm{d}^2}{\mathrm{d}t^2} m[\widetilde{u}, w] + \mathrm{D}_u a(u_0)[\widetilde{u}, w] = \widetilde{l}[w]$$

Dependency on u_0 (assuming know constitutive law and parameters):

$$\mathrm{D}_u a(u_0)[\widetilde{u}, w] = \int_{\hat{\Omega}} \underbrace{\mathrm{D}_{\boldsymbol{u}} \boldsymbol{e}(\boldsymbol{u}_0)[\widetilde{u}] : \mathrm{D}_{\boldsymbol{e}} \boldsymbol{\Sigma}(\boldsymbol{e}_0) : \mathrm{D}_{\boldsymbol{u}} \boldsymbol{e}(\boldsymbol{u}_0)[\boldsymbol{w}]}_{\text{“}\varepsilon(\widetilde{u}) : \boldsymbol{C} : \varepsilon(w)\text{”}} \, \mathrm{d}\hat{\Omega} + \int_{\hat{\Omega}} \underbrace{\boldsymbol{\Sigma}(\boldsymbol{e}_0) : \mathrm{D}^2_u \boldsymbol{e}[\widetilde{\boldsymbol{u}}, \boldsymbol{w}]}_{\text{geometrical nonlinearity}} \, \mathrm{d}\hat{\Omega}$$

Through the strain tensor and the stress tensor (for an arbitrary hyperelastic law):

$$\mathrm{D}_{\boldsymbol{e}} \boldsymbol{\Sigma} = \mathrm{D}^2_{\boldsymbol{e}} W = 4 \sum_{i=1}^{n} \frac{\partial W}{\partial I_i} \frac{\partial^2 I_i}{\partial \boldsymbol{C} \partial \boldsymbol{C}} + 4 \sum_{i,j=1}^{n} \frac{\partial^2 W}{\partial I_i \partial I_j} \frac{\partial I_i}{\partial \boldsymbol{C}} \otimes \frac{\partial I_j}{\partial \boldsymbol{C}}$$

Descent methods such as Full Waveform Inversion requires the tangent dynamics for computing an adjoint model. Virieux et al. 2014

Further differentiation of our direct model would require unwieldy operators as

$$\mathrm{D}^3_{\boldsymbol{e}} W = 8 \sum_{i,j,k=1}^{n} \left[\frac{\partial^3 W}{\partial I_i \partial I_j \partial I_k} \frac{\partial I_i}{\partial \boldsymbol{C}} \otimes \frac{\partial I_j}{\partial \boldsymbol{C}} \otimes \frac{\partial I_k}{\partial \boldsymbol{C}} \right] + 8 \sum_{i,j,k=1}^{n} \frac{\partial^2 W}{\partial I_i \partial I_j} \left[\frac{\partial^2 I_i}{\partial \boldsymbol{C} \partial \boldsymbol{C}} \otimes \frac{\partial I_j}{\partial \boldsymbol{C}} + \cdots \right].$$

Derivative-free methods are preferred.

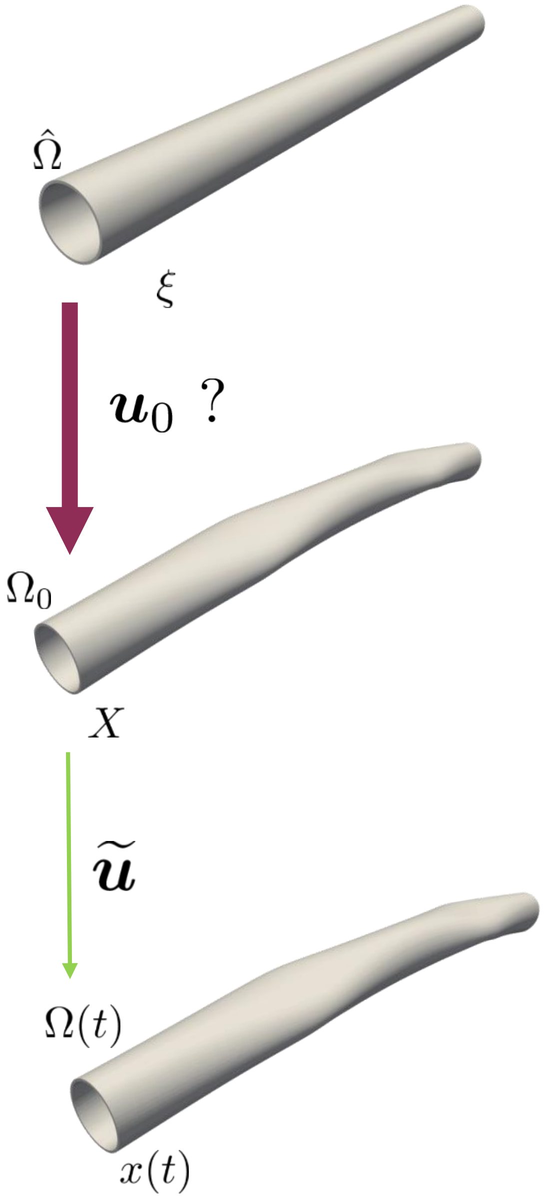

Direct model: $$\frac{\mathrm{d}^2}{\mathrm{d}t^2} m[\widetilde{u}, w] + \mathrm{D}_u a(u_0)[\widetilde{u}, w] = \widetilde{l}[w]$$

The deformation sought u_0 is the result of a mechanical loading / solution of a quasi-static nonlinear problem

$$a(u_0)[w] = l_0(w).$$

Decomposing the deformation with the eigenmodes of a(0)

$$\boldsymbol{u}_0(\boldsymbol{\xi}) = \sum_{i=1}^{N_\theta} u_{i,0} \boldsymbol{\Psi}_i(\boldsymbol{\xi})$$

we can significantly reduce the size of the parametric space to be reconstructed by reconstructing the coeficients $u_0^{(i)}$ with N_θ << Number of DoFs.

The parametric space is reduced and a selection of eigenmodes can be made from a first guess or sensitivity analysis.

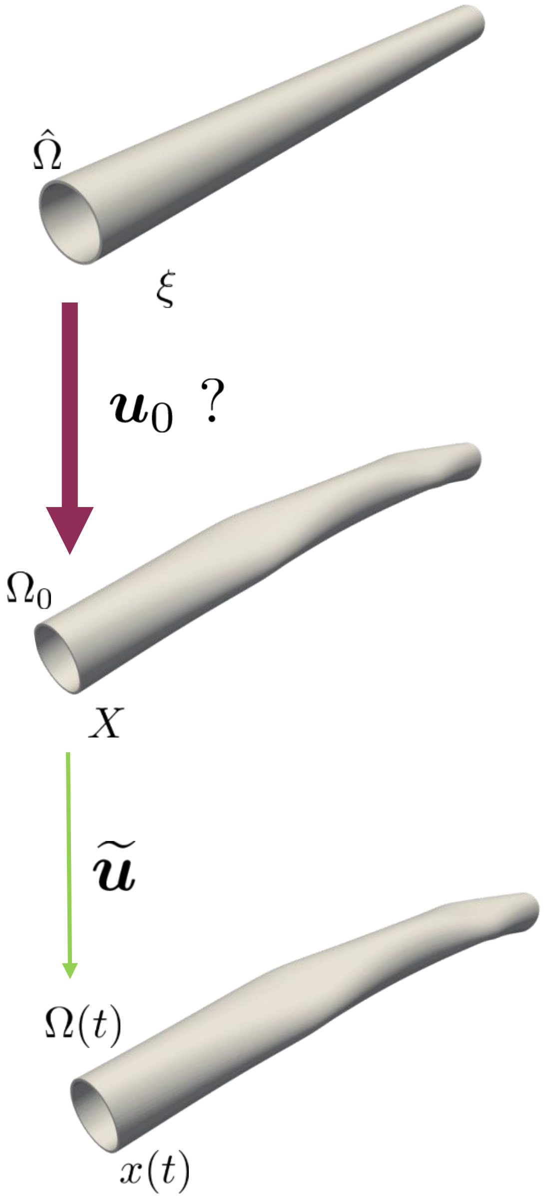

Variational Method

$$\begin{cases} \dfrac{\mathrm{d}}{\mathrm{d}t} p(t) + \mathrm{D}_u A^* \, p(t) = -\mathrm{D}_u C^* \big(y(t) - C(\widetilde{u}(t))\big), \\ p(T) = 0, \end{cases}$$

$$\mathrm{D}\mathcal{J}(u_0) = \mathbb{P}_{u_0}^{-1} u_0 - p(0).$$

Sequential Method

$$\begin{cases} \dfrac{\mathrm{d}}{\mathrm{d}t} \widehat{z}(t) = A(\widehat{z}(t)) + G(t)(y(t) - C(\widetilde{u}(t))), \\ \widehat{z}(0) = z_0, \end{cases}$$

$$\mathrm{z}(\mathrm{T})$$

- With a reduced parametric space, the **Reduced Order Unscented Kalman Filter (ROUKF)** was chosen as the derivative-free method.
- Seem as a derivative-free version of the Extended Kalman Filter, where the propagation of the covariance is done empirically instead of applying the tangent dynamics.

Reduced-Order Unscented Kalman Filter

Sampling:

$$Z_n^{(i)+} = Z_n^+ + L_n \sqrt{U_n^{-1}} I^{(i)} \qquad i \in [1, N_\theta + 1]$$

Prediction:

$Z_n^{(1)+}$ $\quad$ $Z_n^{(2)+}$ $\quad$ $Z_n^{(N_\theta+1)+}$

$$\Psi_{n+1|n}(Z_n^{(1)+}) \qquad \Psi_{n+1|n}(Z_n^{(2)+}) \qquad \cdots \qquad \Psi_{n+1|n}(Z_n^{(N_\theta+1)+})$$

$Z_{n+1}^{(1)-}$ $\quad$ $Z_{n+1}^{(2)-}$ $\quad$ $Z_{n+1}^{(N_\theta+1)-}$

Correction:

$$\begin{aligned}
Z_{n+1}^- &= E_\alpha(Z_{n+1}^{(i)-}) \\
L_{n+1} &= [Z_{n+1}^{*-}] D_\alpha [I^*]^\intercal \\
U_{n+1} &= \mathbb{1} + (CL)_{n+1}^* (CL)_{n+1} \\
Z_{n+1}^+ &= Z_{n+1}^- \\
&\quad + L_{n+1} U_{n+1}^{-1} (CL)_{n+1}^* (y_{n+1} - C E_\alpha(Z_{n+1}^{*+}))
\end{aligned}$$

Moireau and Chapelle 2011

Extended state:

$$Z_n = \begin{pmatrix} \widetilde{u}_n \\ \widetilde{v}_n \\ \vec{u}_{0,n} \end{pmatrix}$$

Forward operator:

$$\Psi_{n+1|n}(Z_n)$$

Covariance:

$$U^{-1}$$

Particles matrix:

$$[Z_n^*] = \begin{pmatrix} Z_n^{(1)} & Z_n^{(2)} & \cdots & Z_n^{(N_\theta+1)} \end{pmatrix}$$

Sigma points and weights matrix:

$$[I^*] \qquad D_\alpha = \begin{pmatrix} \alpha_1 & & \\ & \ddots & \\ & & \alpha_{N_\theta+1} \end{pmatrix}$$

Reduced-Order Unscented Kalman Filter

Sampling:

$$Z_n^{(i)+} = Z_n^+ + L_n \sqrt{U_n^{-1}} I^{(i)} \qquad i \in [1, N_\theta + 1]$$

Prediction:

$Z_n^{(1)+}$ $\quad$ $Z_n^{(2)+}$ $\quad$ $Z_n^{(N_\theta+1)+}$

$\Psi_{n+1|n}(Z_n^{(1)+})$ $\quad$ $\Psi_{n+1|n}(Z_n^{(2)+})$ $\quad \cdots \quad$ $\Psi_{n+1|n}(Z_n^{(N_\theta+1)+})$

$Z_{n+1}^{(1)-}$ $\quad$ $Z_{n+1}^{(2)-}$ $\quad$ $Z_{n+1}^{(N_\theta+1)-}$

Correction:

$$\begin{aligned}
Z_{n+1}^- &= E_\alpha(Z_{n+1}^{(i)-}) \\
L_{n+1} &= [Z_{n+1}^{*-}] D_\alpha [I^*]^\intercal \\
U_{n+1} &= \mathbb{1} + (CL)_{n+1}^* (CL)_{n+1} \\
Z_{n+1}^+ &= Z_{n+1}^- \\
&\quad + L_{n+1} U_{n+1}^{-1} (CL)_{n+1}^* (y_{n+1} - C E_\alpha(Z_{n+1}^{*+}))
\end{aligned}$$

Moireau and Chapelle 2011

- Uncertainty only in u_0.
- Iteration by time-step.
- Particles are evaluated in parallel.
- Propagates the covariance.

Reduced-Order Unscented Kalman Filter

Sampling:

$$Z_n^{(i)+} = Z_n^+ + L_n \sqrt{U_n^{-1}} I^{(i)}$$

$i \in [1, N_\theta + 1]$

Prediction:

$Z_n^{(1)+}$ $Z_n^{(2)+}$ $Z_n^{(N_\theta+1)+}$

$$\Psi_{n+1|n}(Z_n^{(1)+}) \quad \Psi_{n+1|n}(Z_n^{(2)+}) \quad \cdots \quad \Psi_{n+1|n}(Z_n^{(N_\theta+1)+})$$

$Z_{n+1}^{(1)-}$ $Z_{n+1}^{(2)-}$ $Z_{n+1}^{(N_\theta+1)-}$

Correction:

$$\begin{aligned}
Z_{n+1}^- &= E_\alpha(Z_{n+1}^{(i)-}) \\
L_{n+1} &= [Z_{n+1}^{*-}] D_\alpha [I^*]^\intercal \\
U_{n+1} &= \mathbb{1} + (CL)_{n+1}^* (CL)_{n+1} \\
Z_{n+1}^+ &= Z_{n+1}^- \\
&\quad + L_{n+1} U_{n+1}^{-1} (CL)_{n+1}^* (y_{n+1} - C E_\alpha(Z_{n+1}^{*+}))
\end{aligned}$$

Moireau and Chapelle 2011

- Eigenmodes are stored and the non-assembled aspect allows inexpensive change of parameter.
- Attention must be given to the range explored by the particles to assure stability. This is done when choosing the initial covariance.

$$U_0 = \mathbb{P}_{u_0}$$

The initial components covariance of the set of eigenmodes are chosen from a u_0 *a priori*.

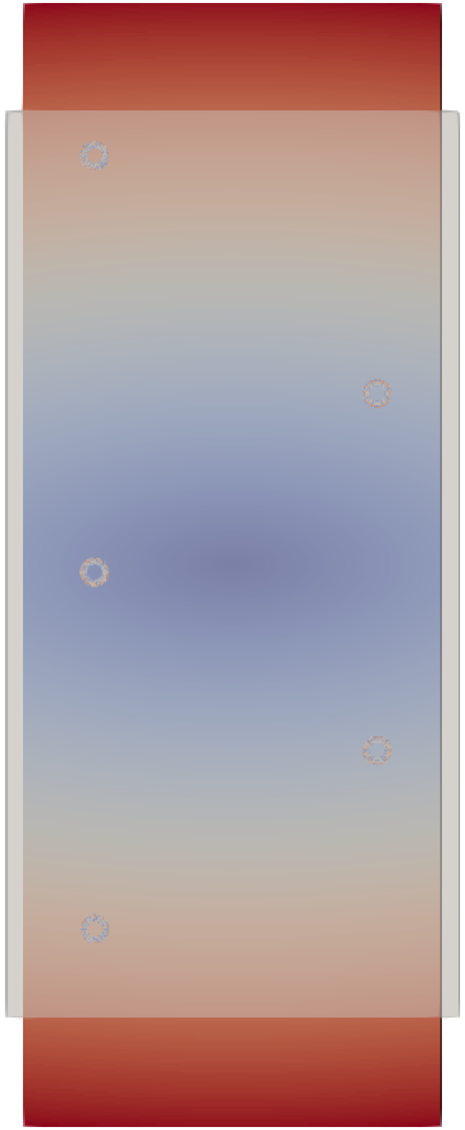

Transducers, natural state and target deformed state.
(300x deformation scale)

- Dimensions: 600 x 300 x 6.35 mm
- Measurements: 5 integration patches (radial).
- Excitation: 200kHz 5-cycles.
- Noise: 0.1%
- 180µs simulation time.
- 120 Smallest eigenvalues pairs computed.

Example of measured signal:

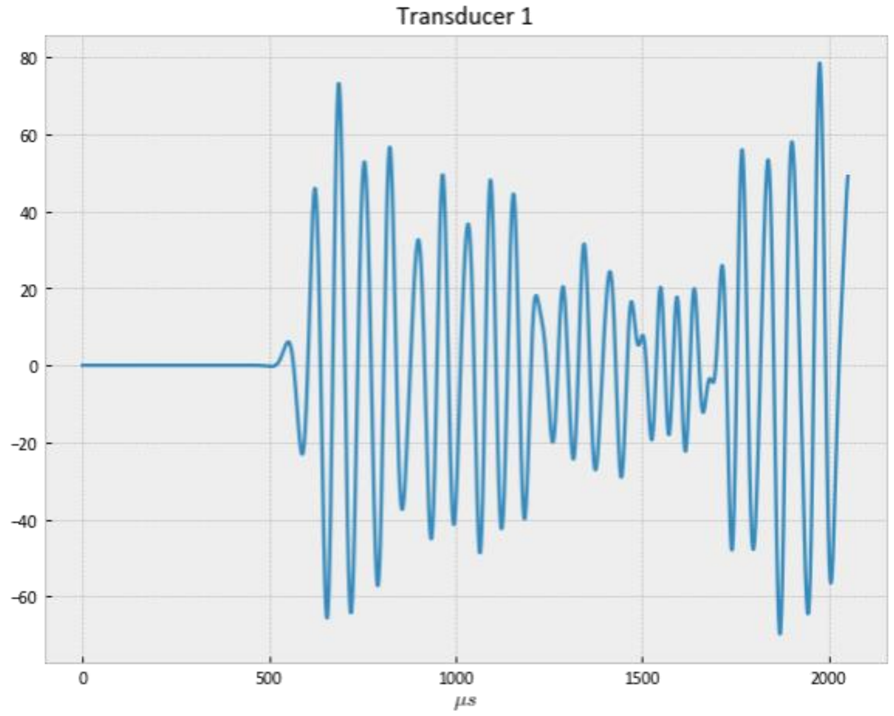

Obs. operator: $$C_i(\widetilde{u}(t)) = \int_{\Gamma_i} \widetilde{\boldsymbol{u}}(t) \cdot \boldsymbol{s}_i \, \mathrm{d}\Gamma, \quad i \in [1,5]$$

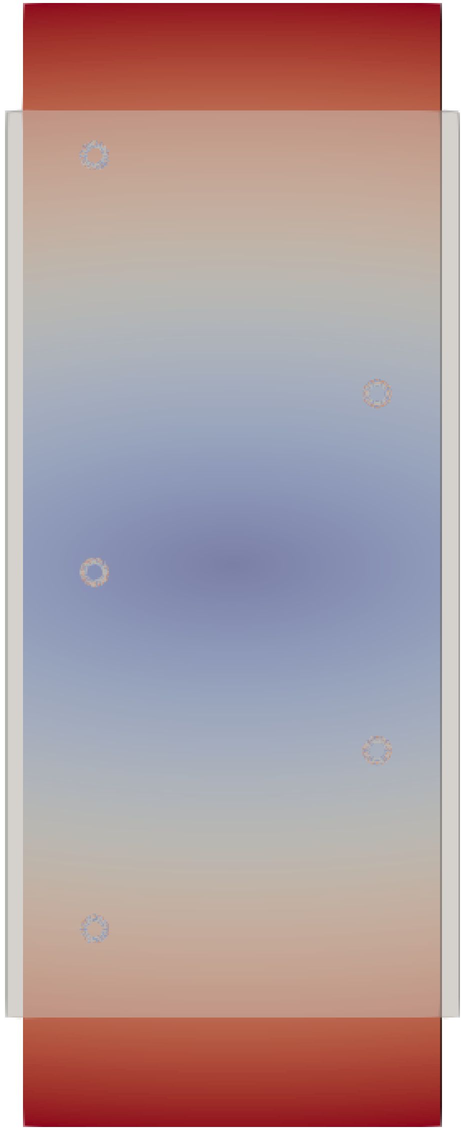

Transducers, natural state and target deformed state.
(300x deformation scale)

Target wavefield

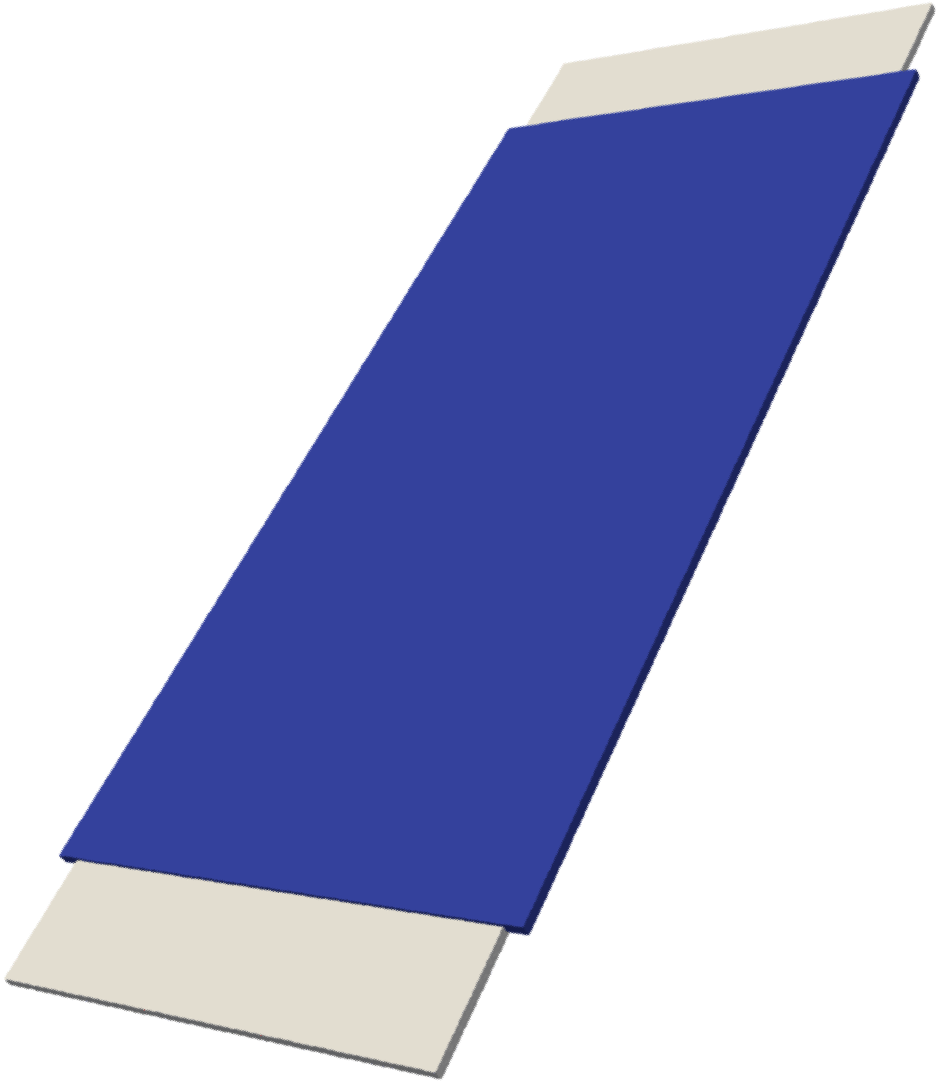

(300x deformation scale)

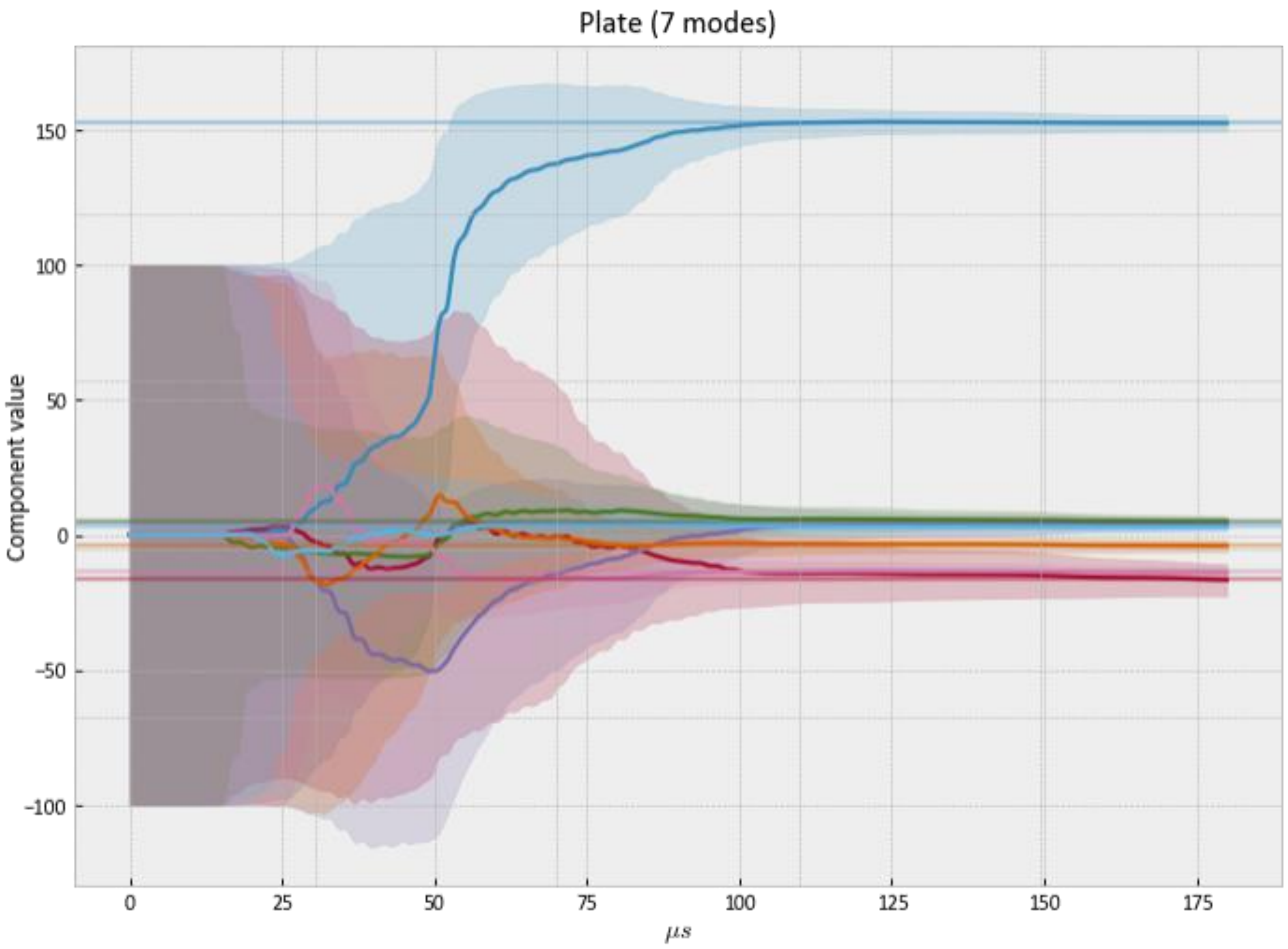

Mode components estimation through the simulation time.

- Dimensions: 2.94m, Ø 0.1973m and 8mm
- Measurements: 24 integration patches (radial).
- Excitation: 30kHz 5-cycles.
- Noise: 0.1%
- 1400µs simulation time.
- 100 smallest eigenvalues pairs computed.

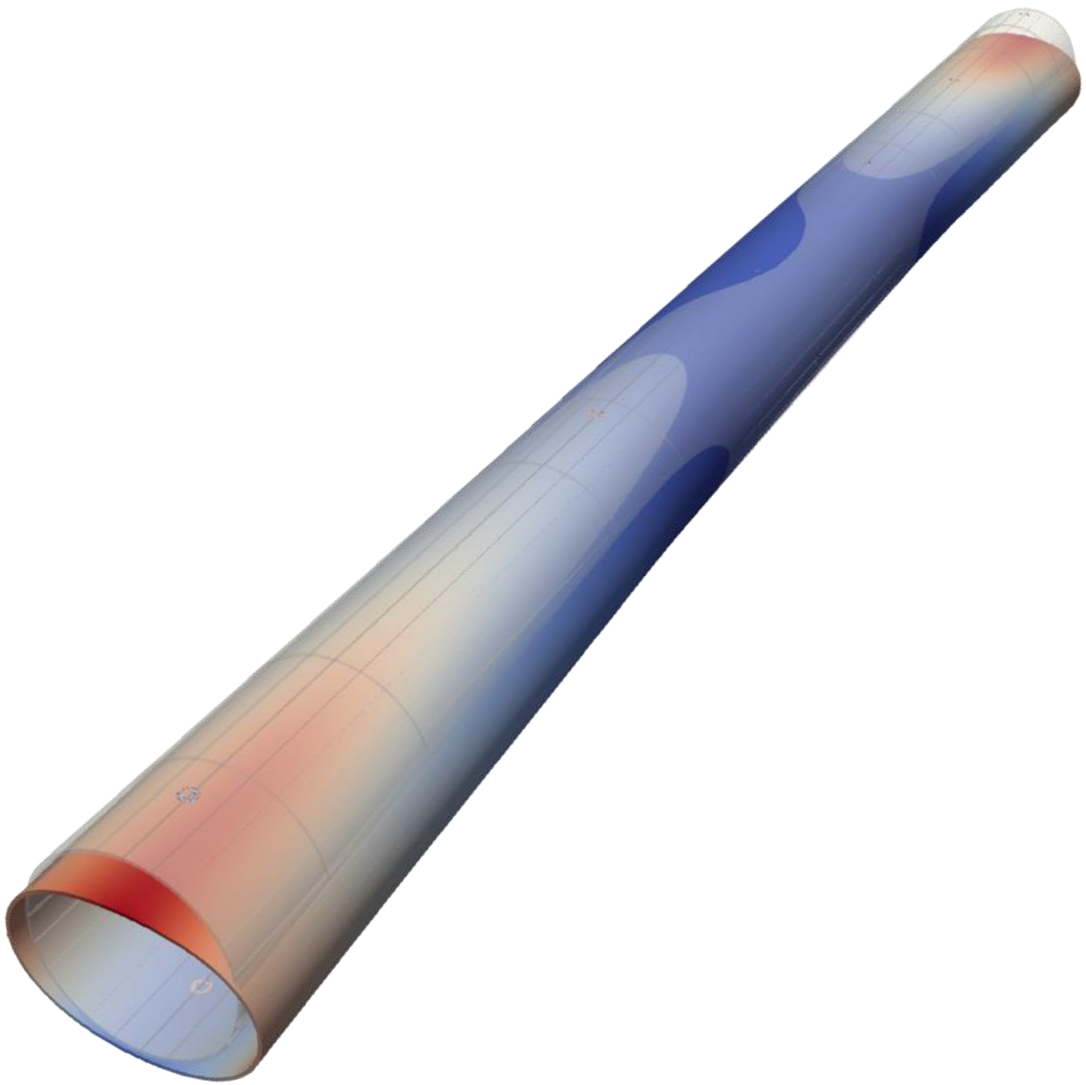

Transducers, natural state and target deformed state.
(3x deformation scale)

Example of measured signal:

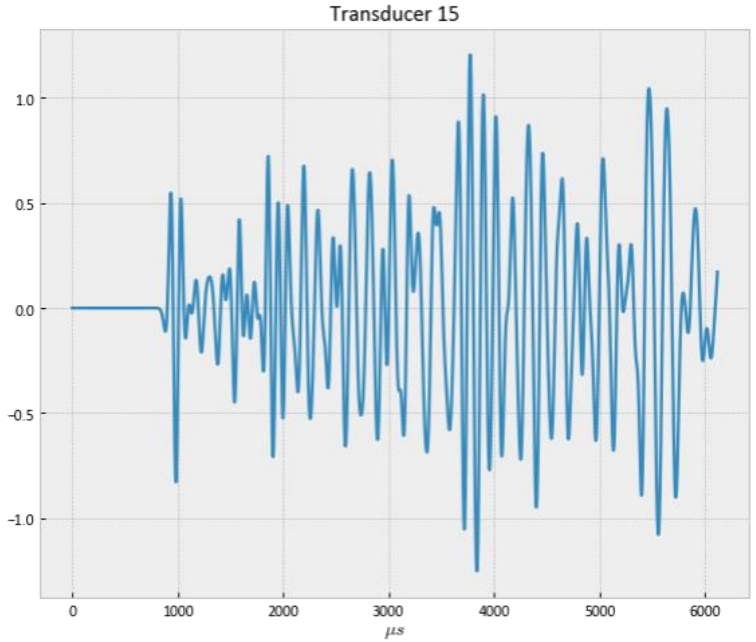

Obs. operator: $$C_i(\widetilde{u}(t)) = \int_{\Gamma_i} \widetilde{\boldsymbol{u}}(t) \cdot \boldsymbol{s}_i \, \mathrm{d}\Gamma, \quad i \in [1, 24]$$

Iterated case: Estimation is redone with different *a priori*.

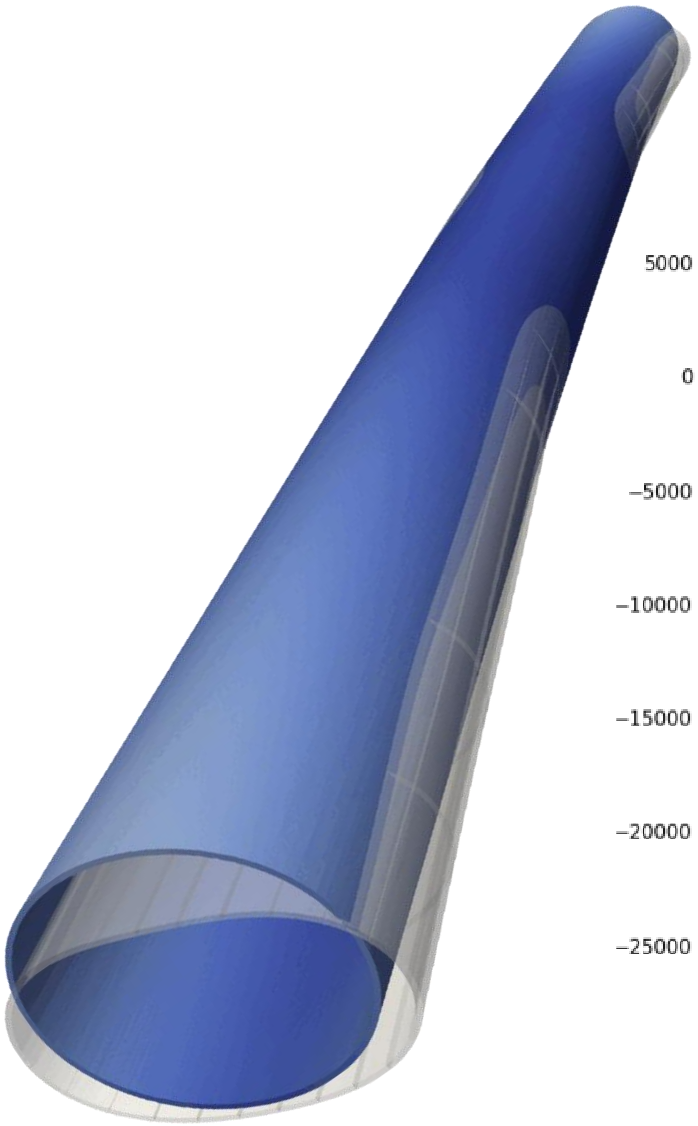

Reconstruction
(3x deformation scale)

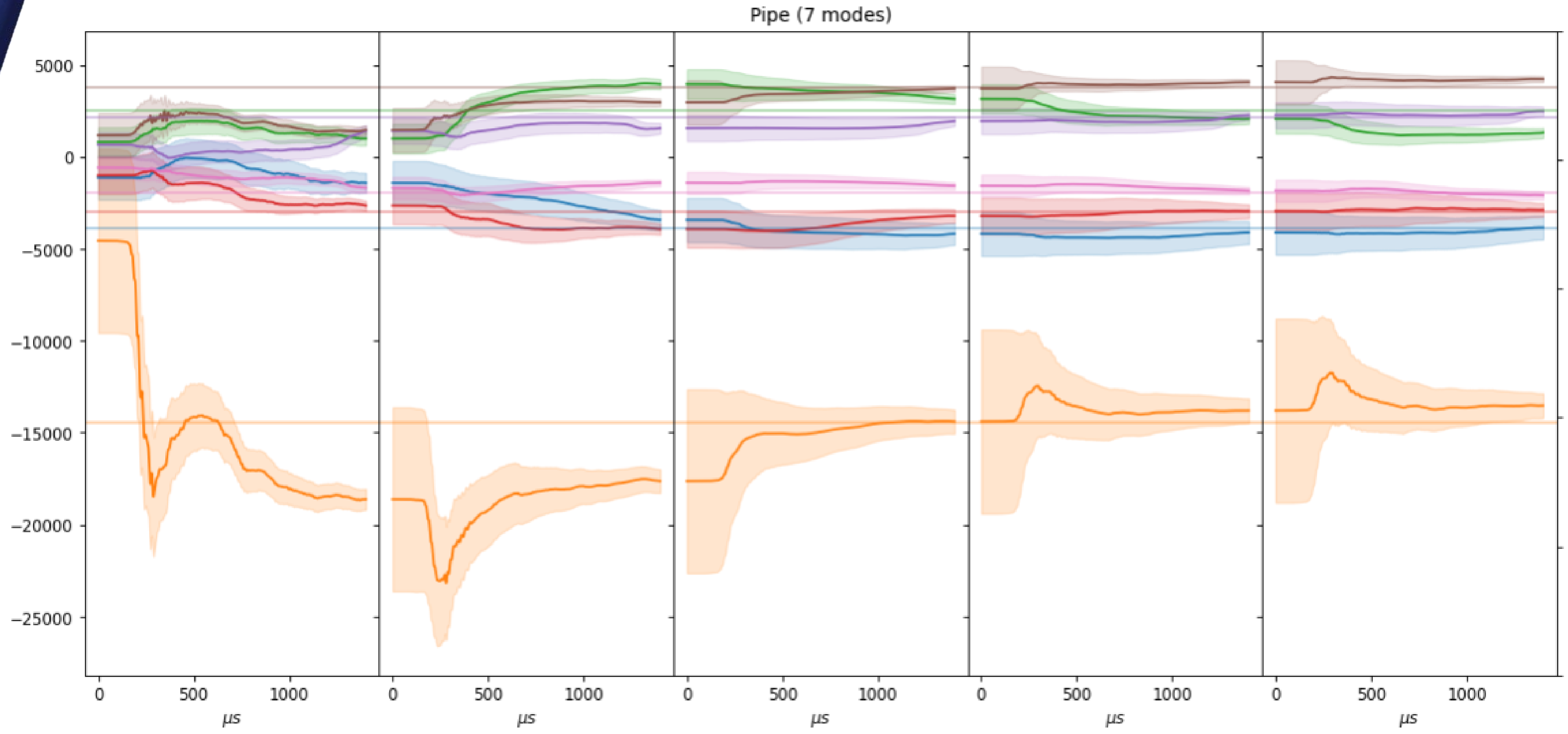

Mode components estimation repeated 5x through the simulation time.

Conclusions

- A **mechanical and numerical model** was presented for **wave propagation on loaded structures**. It comprises arbitrary hyperelastic law and non-buckling load.
- The simulation model was **validated using experimental data**.
- **Reconstruction of loading deformation** of the structure is done using the presented direct model and **Reduced order Kalman Filter** (ROUKF).
- Reconstruction of loading deformation on realistic cases were presented.

Perspectives

- Further studies on the stability of the model and limitation of search range of estimator to **mitigate instability** during inversion.
- Mode selection: **sensitivity analysis** from estimation using observed data; different base with the *a priori*.

Literature and Acknowledgements

- Alexandre Imperiale, and Edouard Demaldent. 2019. "A Macro-Element Strategy Based upon Spectral Finite Elements and Mortar Elements for Transient Wave Propagation Modeling. Application to Ultrasonic Testing of Laminate Composite Materials." International Journal for Numerical Methods in Engineering 119 (10): 964–90.
- Chapelle, Dominique, Anca Ferent, and K. Bathe. 2004. "3D-Shell Elements and Their Underlying Mathematical Model." *Mathematical Models and Methods in Applied Sciences* 14.
- Cohen, Gary C. 2002. *Higher-Order Numerical Methods for Transient Wave Equations*. 1st edition. Scientific Computation. Berlin Heidelberg: Springer-Verlag.
- Dalmora, André, Alexandre Imperiale, Sébastien Imperiale, and Philippe Moireau. 2022. "A Generic Numerical Solver for Modeling the Influence of Stress Conditions on Guided Wave Propagation for SHM Applications." In . American Society of Mechanical Engineers Digital Collection.
- Gandhi, Navneet, Jennifer E Michaels, and Sang Jun Lee. 2012. "Acoustoelastic Lamb Wave Propagation in Biaxially Stressed Plates." The Journal of the Acoustical Society of America 132 (3): 1284–93.
- Joly, Patrick. 2007. "Numerical Methods for Elastic Wave Propagation." In *Waves in Nonlinear Pre-Stressed Materials*, edited by Michel Destrade and Giuseppe Saccomandi, 181–281. CISM Courses and Lectures. Vienna: Springer.
- Maday, Yvon, and Anthony T. Patera. 1989. *Spectral Element Methods for the Incompressible Navier-Stokes Equations*.
- Moireau, Philippe, and Dominique Chapelle. 2011. "Reduced-Order Unscented Kalman Filtering with Application to Parameter Identification in Large-Dimensional Systems." ESAIM: Control, Optimisation and Calculus of Variations 17 (2): 380–405.
- Virieux, J., A. Asnaashari, R. Brossier, L. Métivier, A. Ribodetti, and W. Zhou. 2014. "6. An Introduction to Full Waveform Inversion." In *Encyclopedia of Exploration Geophysics*, R1-1-R1-40. Geophysical References Series. Society of Exploration Geophysicists.

This research was funded by the following project: "GW4SHM" (gw4shm.eu) project from the European Union's Horizon 2020 Research and Innovation program under the Marie Skłodowska-Curie, grant number 860104.

Thank you for your attention

Experimental setup

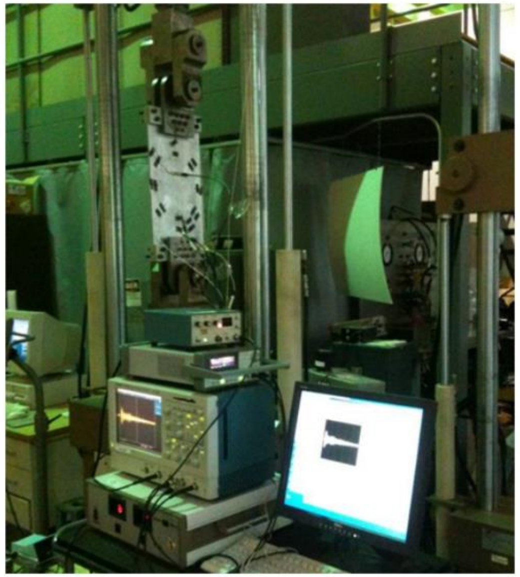

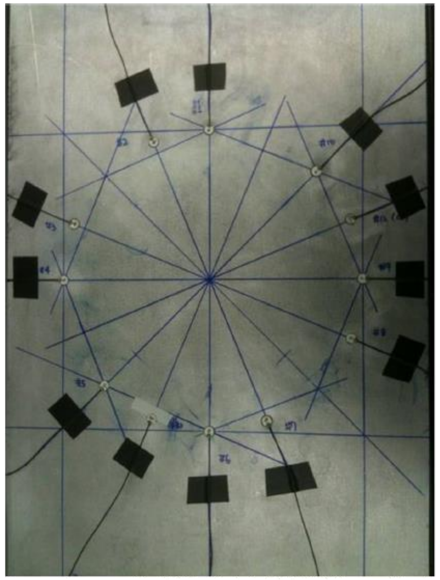

Experimental configuration for measuring velocity changes due to prestresses.

- Frequency: 250khz (S0 mode)
- 610 x 305 x 6.35 mm aluminium plate
- Axial loading from 0MPa to 57.5MPa

Gandhi et al. 2012

Comparing Models

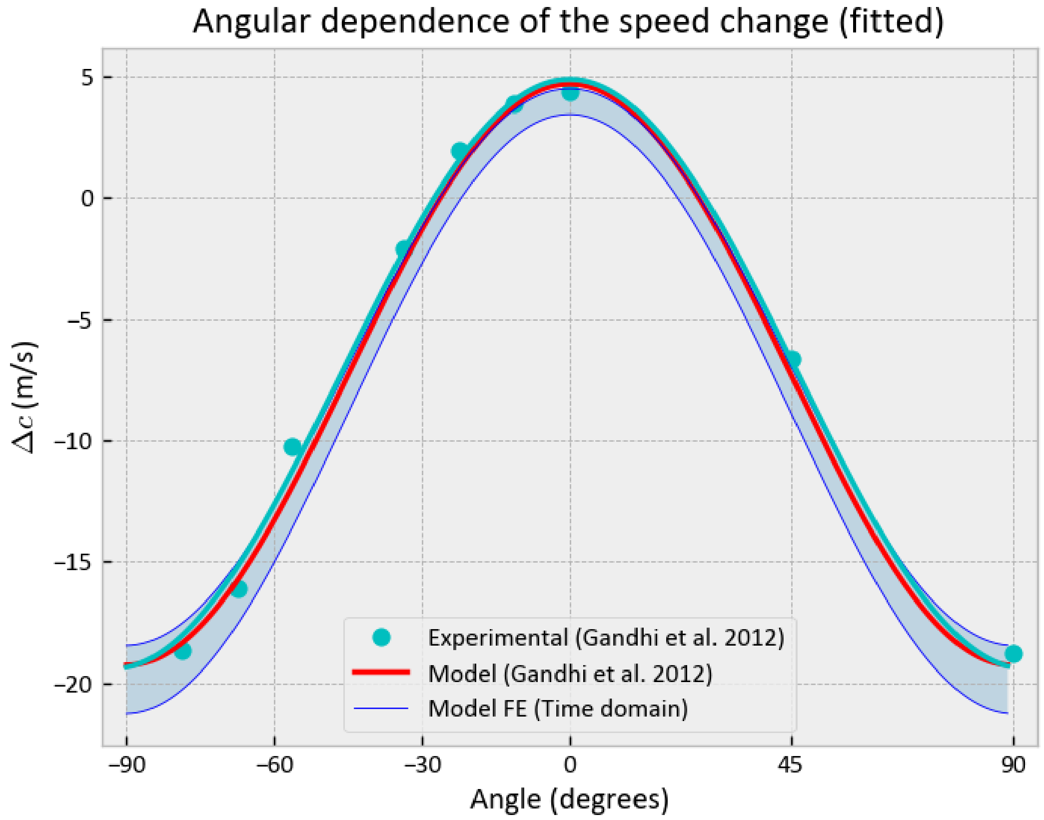

Velocity change (S0 mode) due to prestresses (57.5MPa) relative to the angle of propagation with fitted material parameters.

Composite and stratified materials

Model

Using a transversely isotropic hyperelastic law for each layer it is possible to model stratified composite materials such as CFRP.

$$W = \frac{\mu}{2}(I_1 - 3) - \mu \log \sqrt{I_3} + \frac{\lambda}{2}(\sqrt{I_3} - 2)^2$$
$$+ [\alpha + \beta \log \sqrt{I_3} + \gamma(I_4 - 1)](I_4 - 1) - \frac{\alpha}{2}(I_5 - 1)$$

Bonet, J, and AJ Burton. 1998.

16-ply quasi-isotropic CFRP plate

Dimensions:
900 x 300 x 2 [mm]

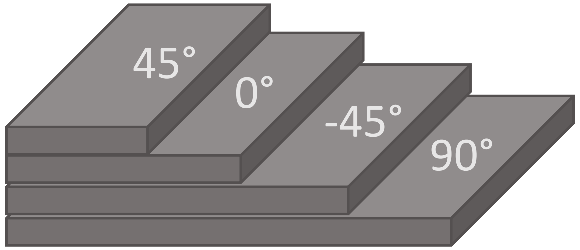

[45°, 0°, -45°, 90°]

$[45°, 0°, -45°, 90°]_{2S}$

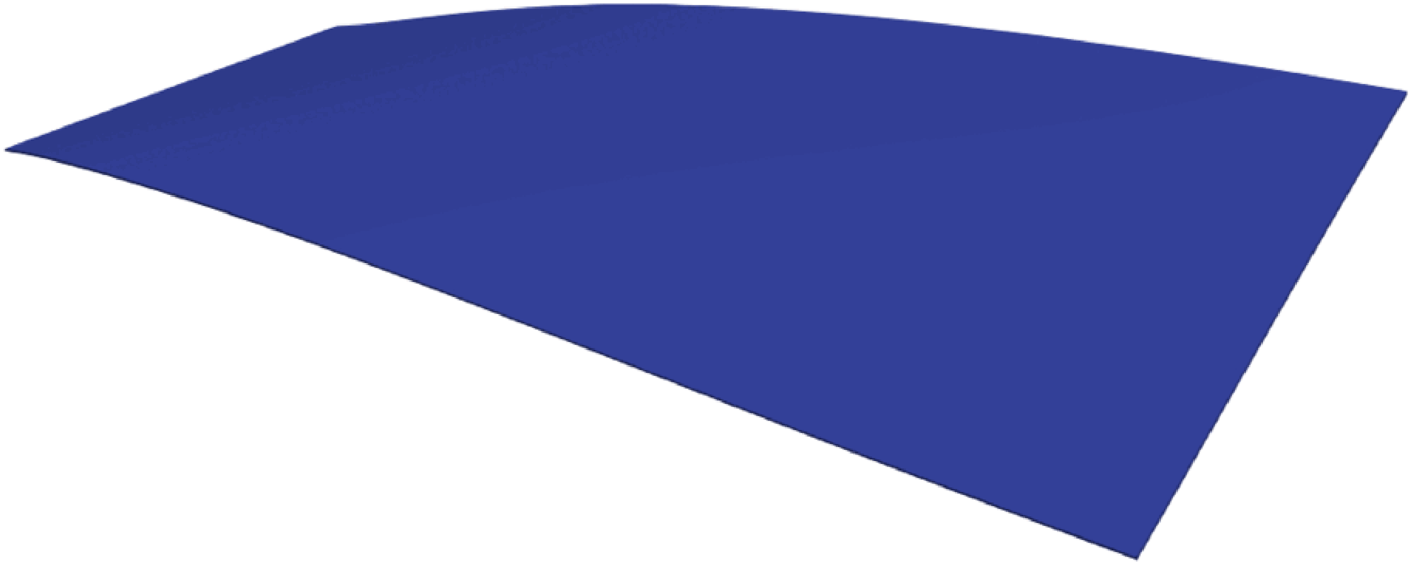

Guided wave propagation in the deformed structure.

- Let us consider $(v^{(i)})_{1\leq i\leq N_s}$ such that

$$\Pi = \sum_{1\leq i\leq N_s} \omega_i v^{(i)} v^{(i)\intercal}$$

- The $(v^{(i)})_{1\leq i\leq N_s}$ can be defined from any generically decomposition of the identy over $(e^{(i)})_{1\leq i\leq N_s}$ with

$$\sum_{1\leq i\leq N_s} \omega_i e^{(i)} e^{(i)\intercal} = \mathbb{1}, \quad v^{(i)} = \sqrt{\Pi} e^{(i)}$$

- Then for any matrix Γ

$$\Gamma\Pi\Gamma^\intercal = \sum_{1\leq i\leq N_s} \omega_i (\Gamma v^{(i)})(\Gamma v^{(i)})^\intercal$$

- If $\Gamma = \, d\varphi(z)$, we have

$$d\varphi(z)\Pi\, d\varphi(z)^\intercal = \sum_{1\leq i\leq N_s} \omega_i (\, d\varphi(z)v^{(i)})(\, d\varphi(z)v^{(i)})^\intercal$$

- Note that $\, d\varphi(z)v \simeq \varphi(z+v) - \varphi(z)$ with equality for linear φ hence

$$d\varphi(z)\Pi\, d\varphi(z)^\intercal \simeq \sum_{1\leq i\leq N_s} \omega_i (\varphi(z+v^{(i)}) - \varphi(z))(\varphi(z+v^{(i)}) - \varphi(z))^\intercal$$

- .. with equality when φ is a linear operator ...

Slide taken from the course
MSE 303 { Data assimilation fundamentals)
Philippe Moireau
Inria
LMS, Ecole Polytechnique,
CNRS, Institut Polytechnique de Paris

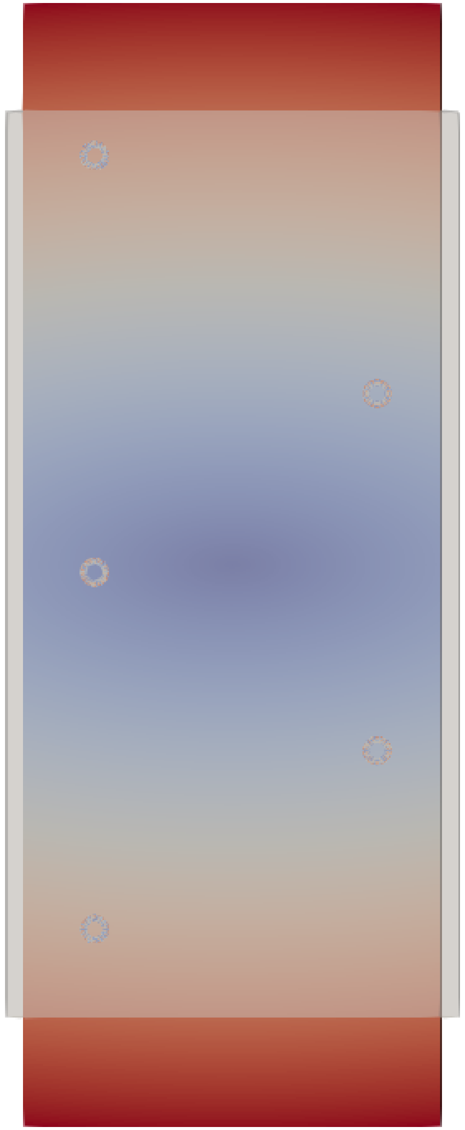

Transducers, natural state and target deformed state.
(300x deformation scale)

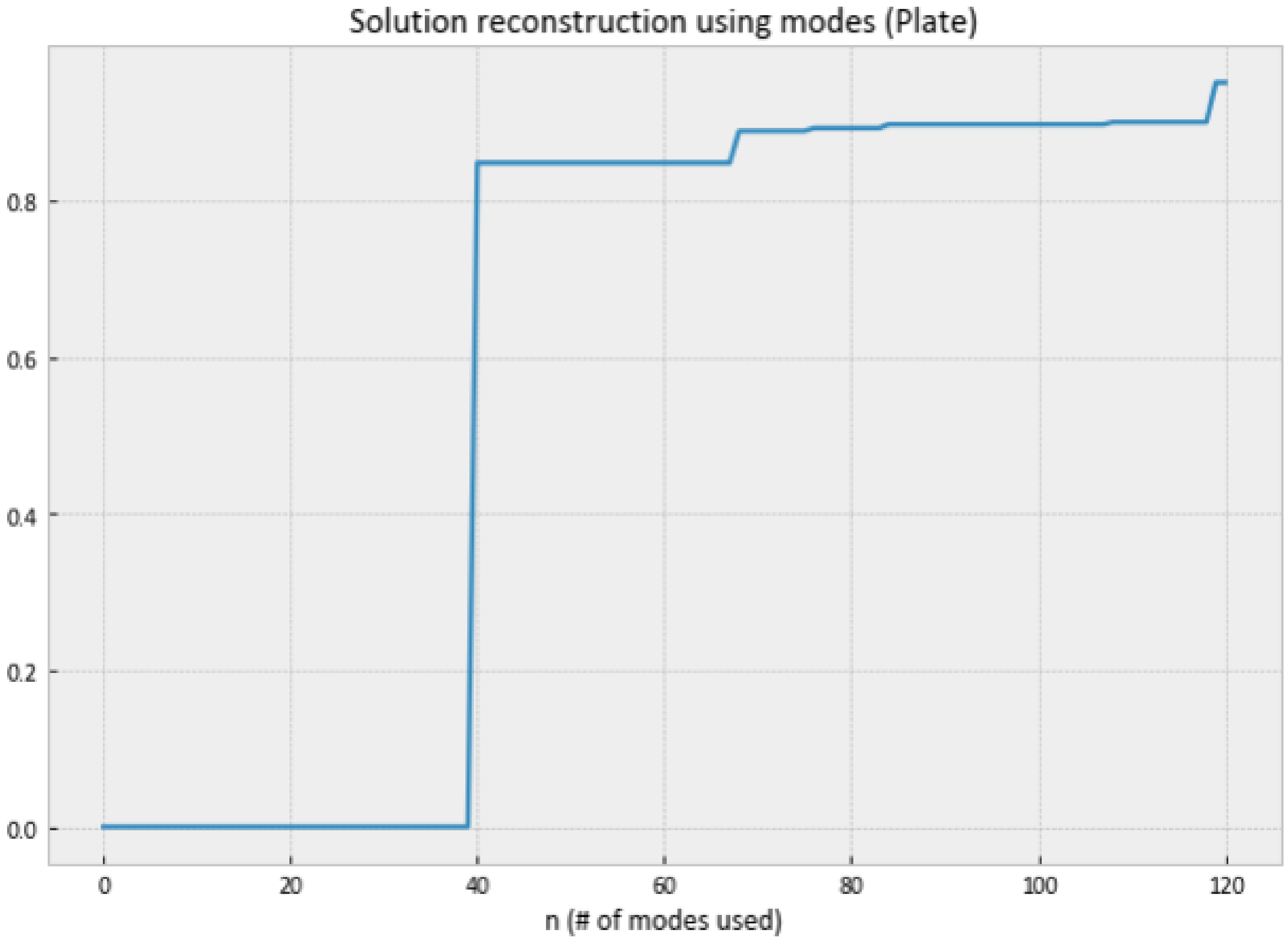

Target deformation reconstruction by number of static-problem eigenmodes used.

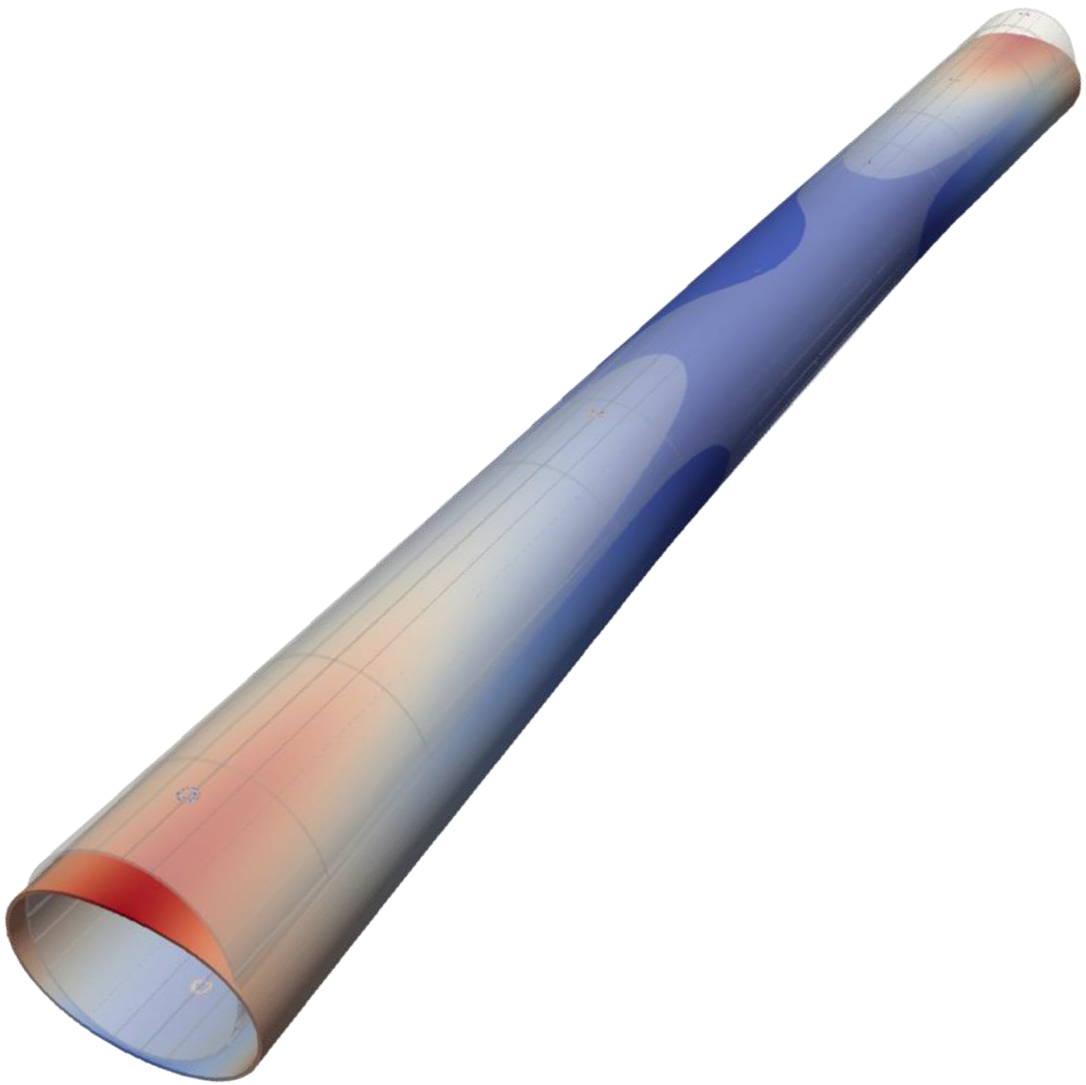

Transducers, natural state and target deformed state.
(3x deformation scale)

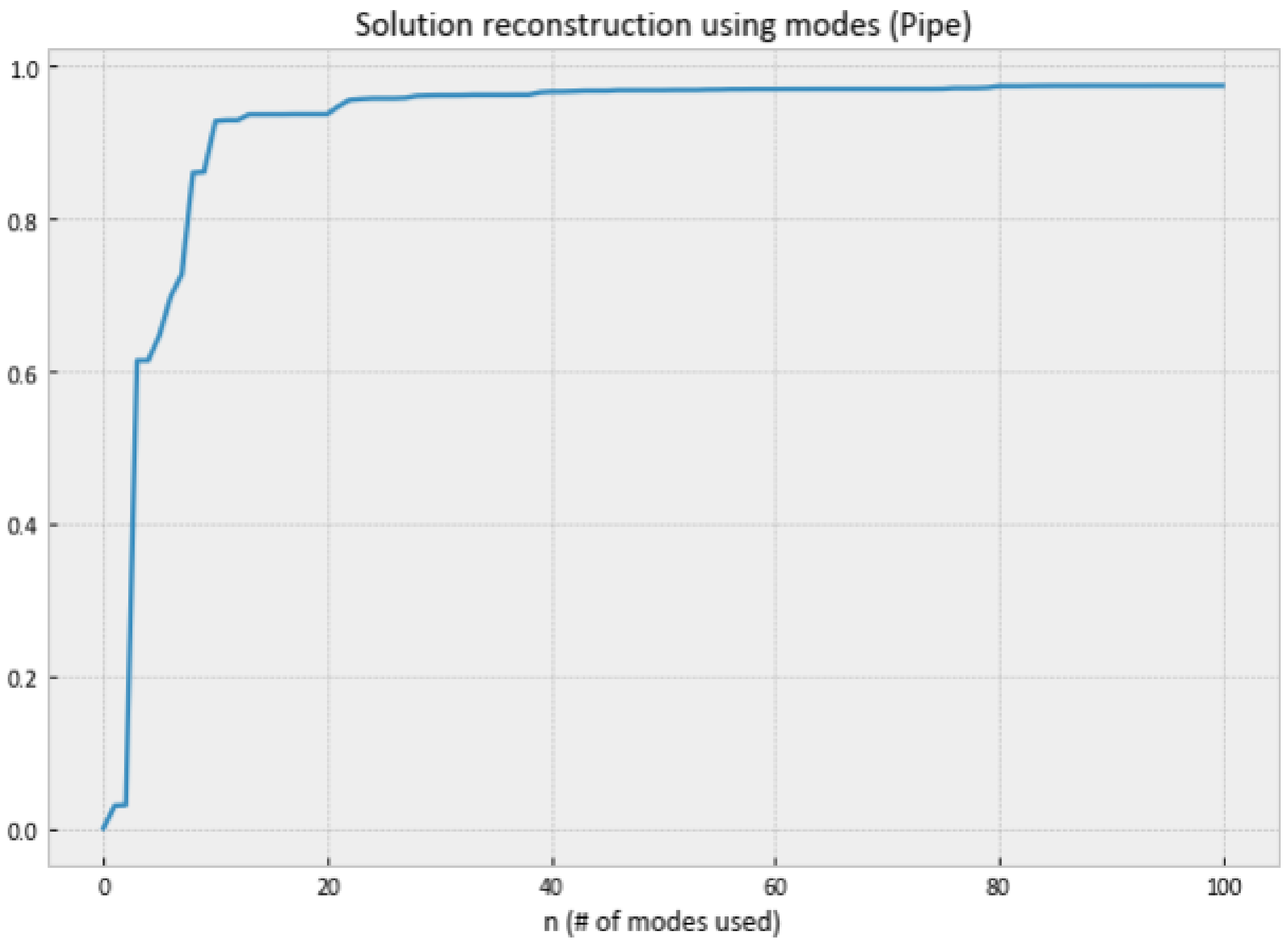

Target deformation reconstruction by number of static-problem eigenmodes used.

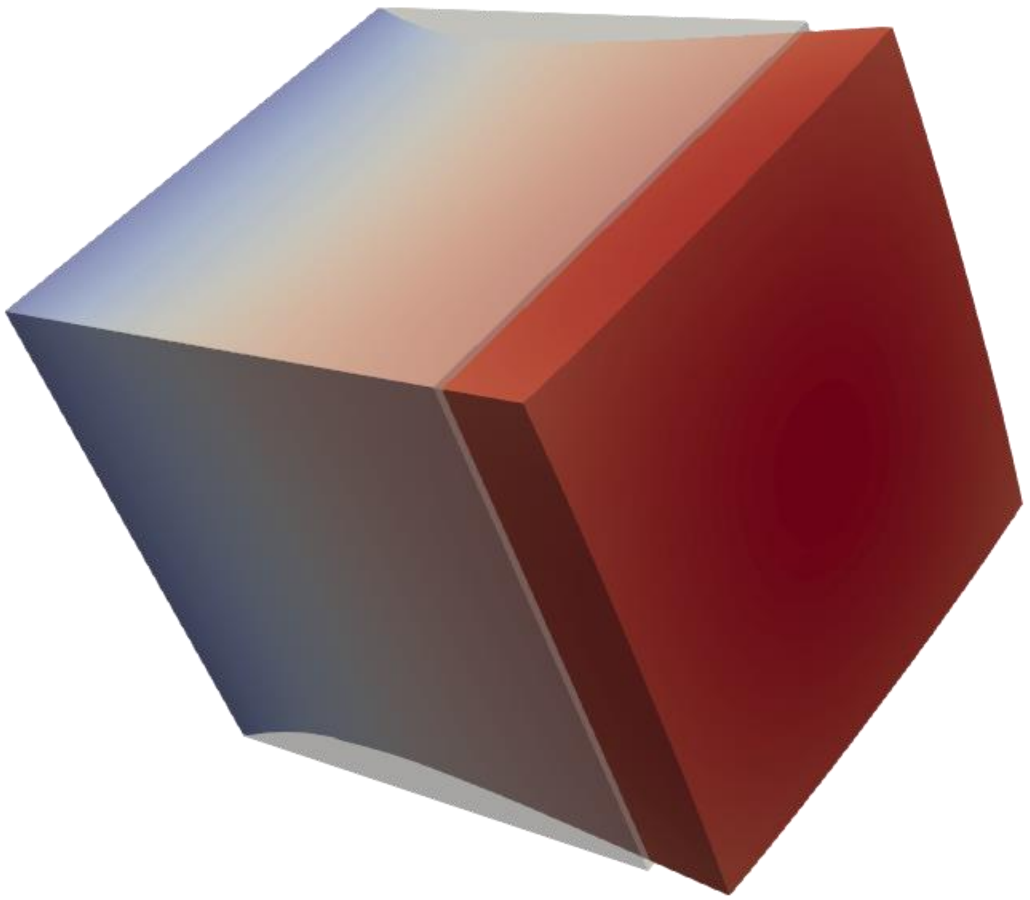

Natural state and target deformed state.
(10x deformation scale)

- Dimensions: 60 x 60 x 60 mm
- Measurements: XYZ solutions at the faces center.
- Excitation: 100kHz 5-cycles at a remaining face.
- Noise: 0.1%
- 100µs simulation time.
- 100 smallest eigenvalues pairs computed.

Example of measured signal:

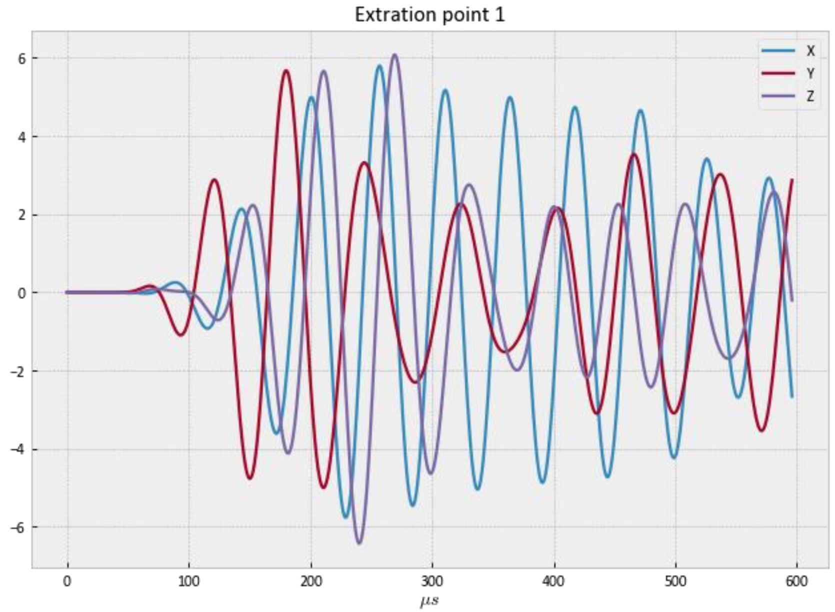

Obs. operator: $$C_{\boldsymbol{i}}(\tilde{u}(t)) = \frac{1}{|\Gamma_i|}\int_{\Gamma_i} \tilde{u}_j(t)\, \mathrm{d}\Gamma, \quad \boldsymbol{i} = (i,j), i \in [1,5], j \in [1,3]$$

Added noise: $$y_j^{\delta,n} = y_j^n + \frac{\delta}{\sqrt{\Delta t}}\chi_j^n \|y_j\|_{L_2} \qquad \|y_j\|_{L_2}^2 = \sum_n^{N_T} \frac{\Delta t}{N_T} y_j^{n\intercal} y_j^n$$

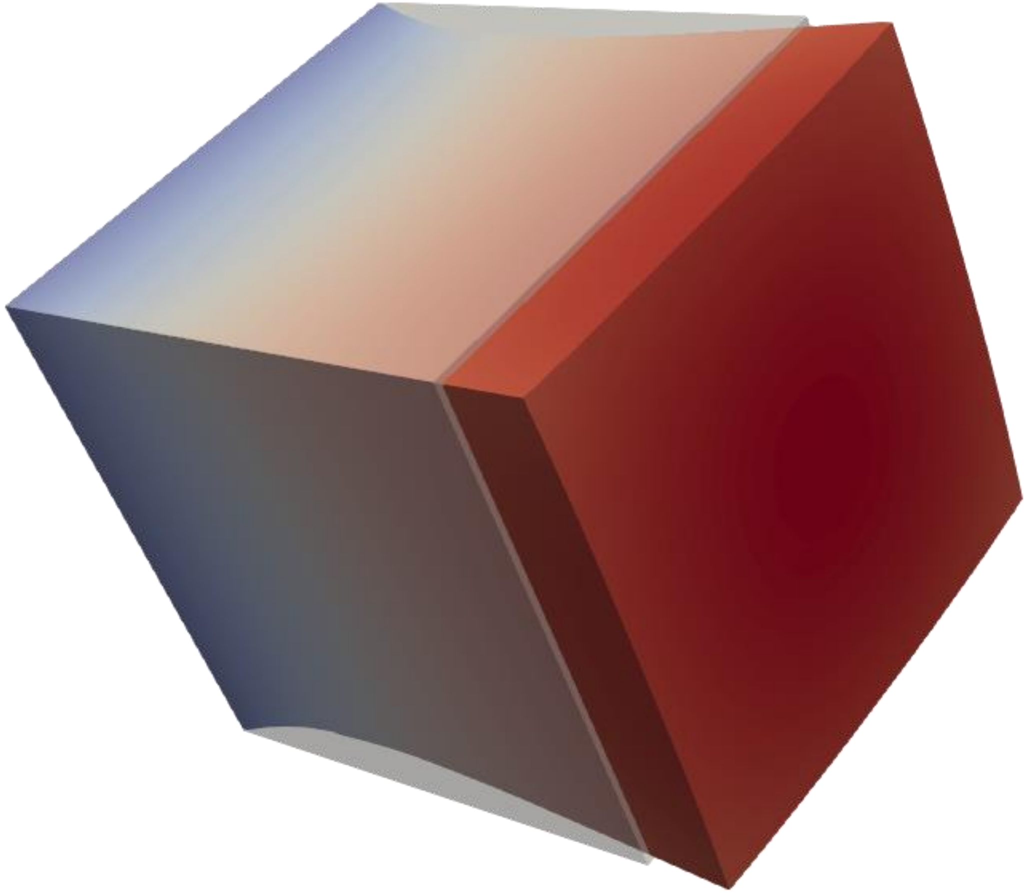

Natural state and target deformed state.
(10x deformation scale)

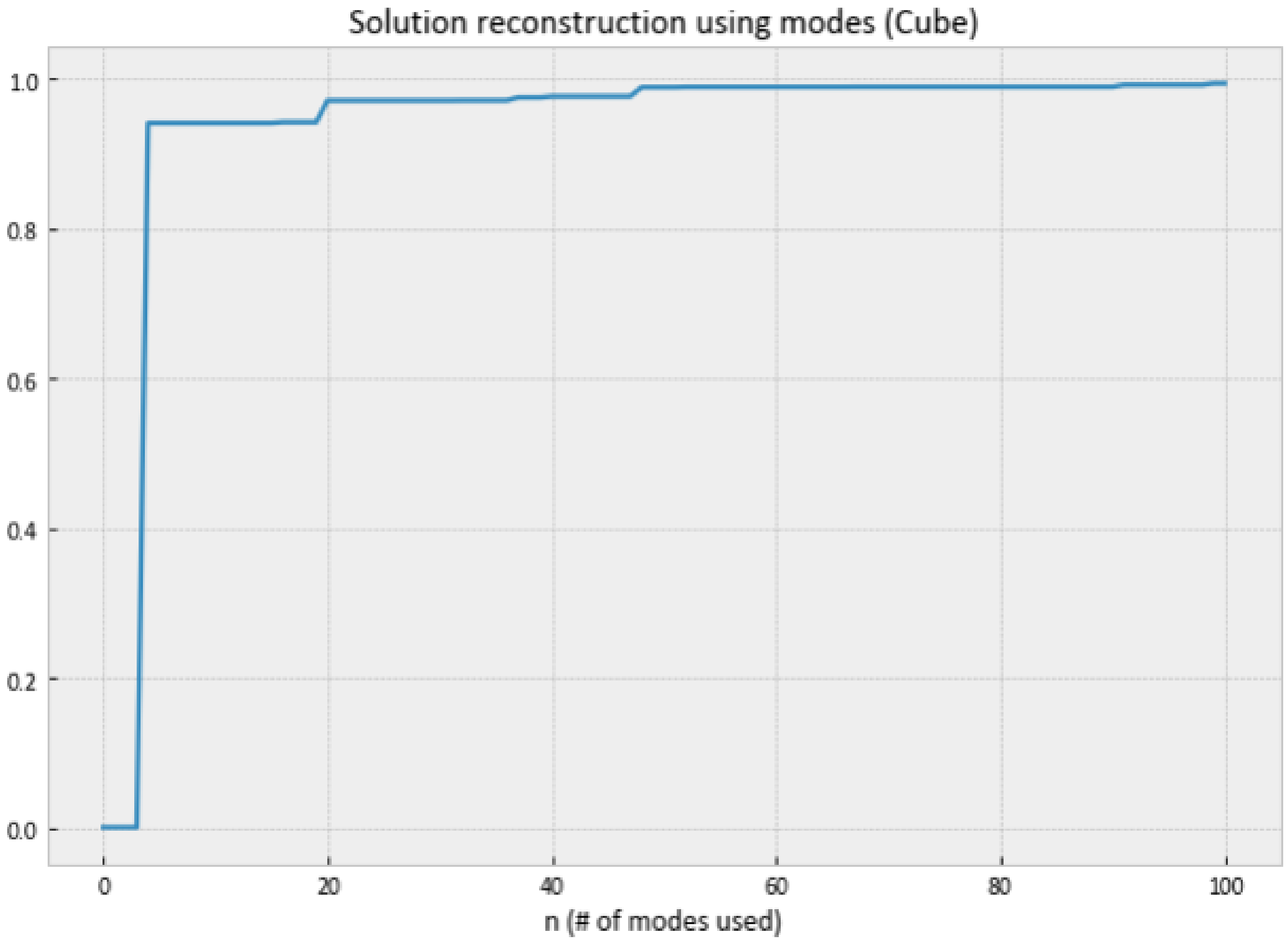

Target deformation reconstruction by number of static-problem eigenmodes used.

$$\text{Plot : } 1 - \frac{\|(u_0 - \sum_{i=0}^{n} u_0^{(i)} \Psi_i)\|_{\mathbb{M}}}{\|u_0\|_{\mathbb{M}}}$$

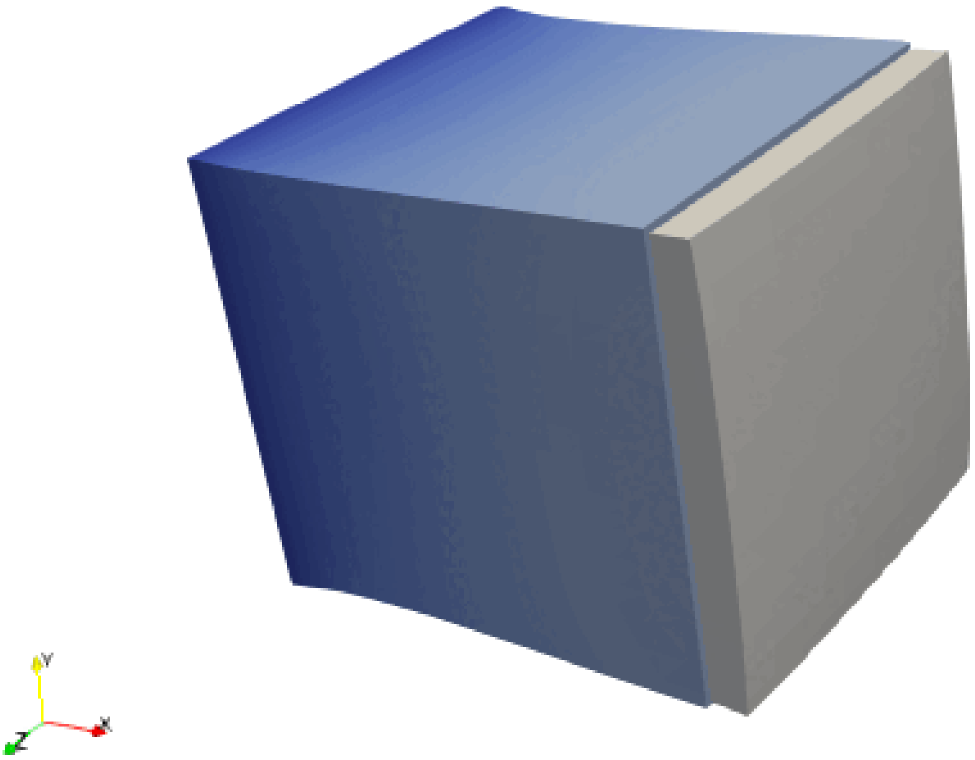

Natural state and target deformed state.
(10x deformation scale)

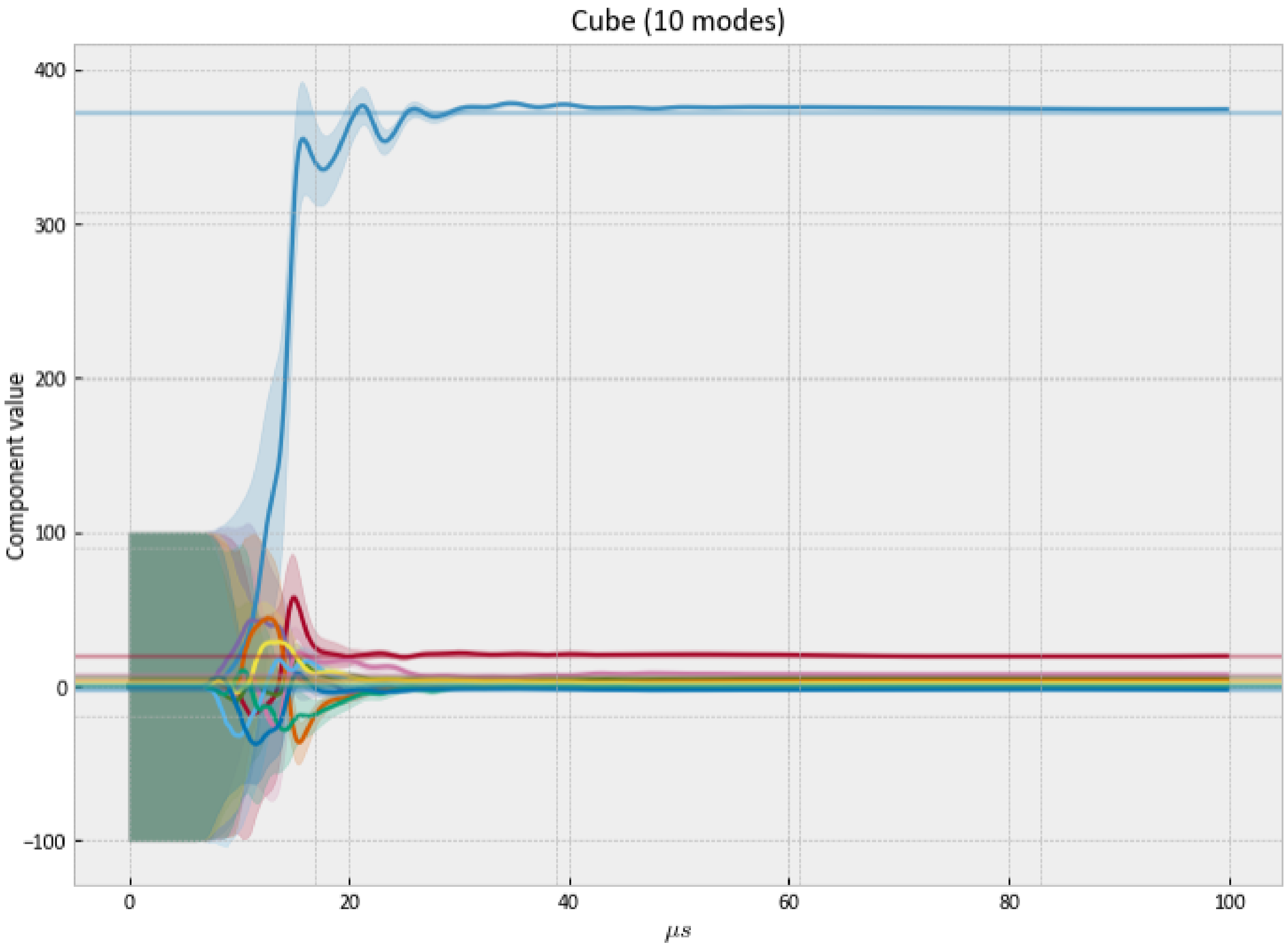

Mode components estimation through the simulation time.

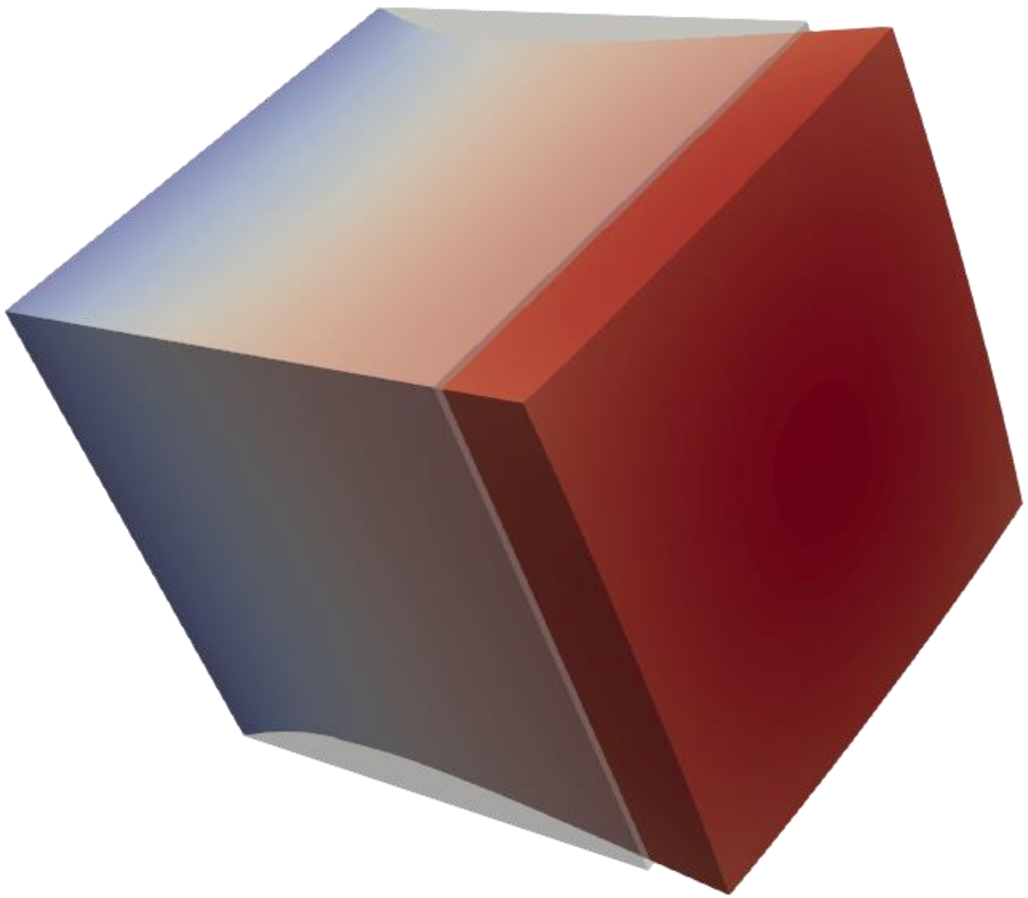

Natural state and target deformed state.
(10x deformation scale)

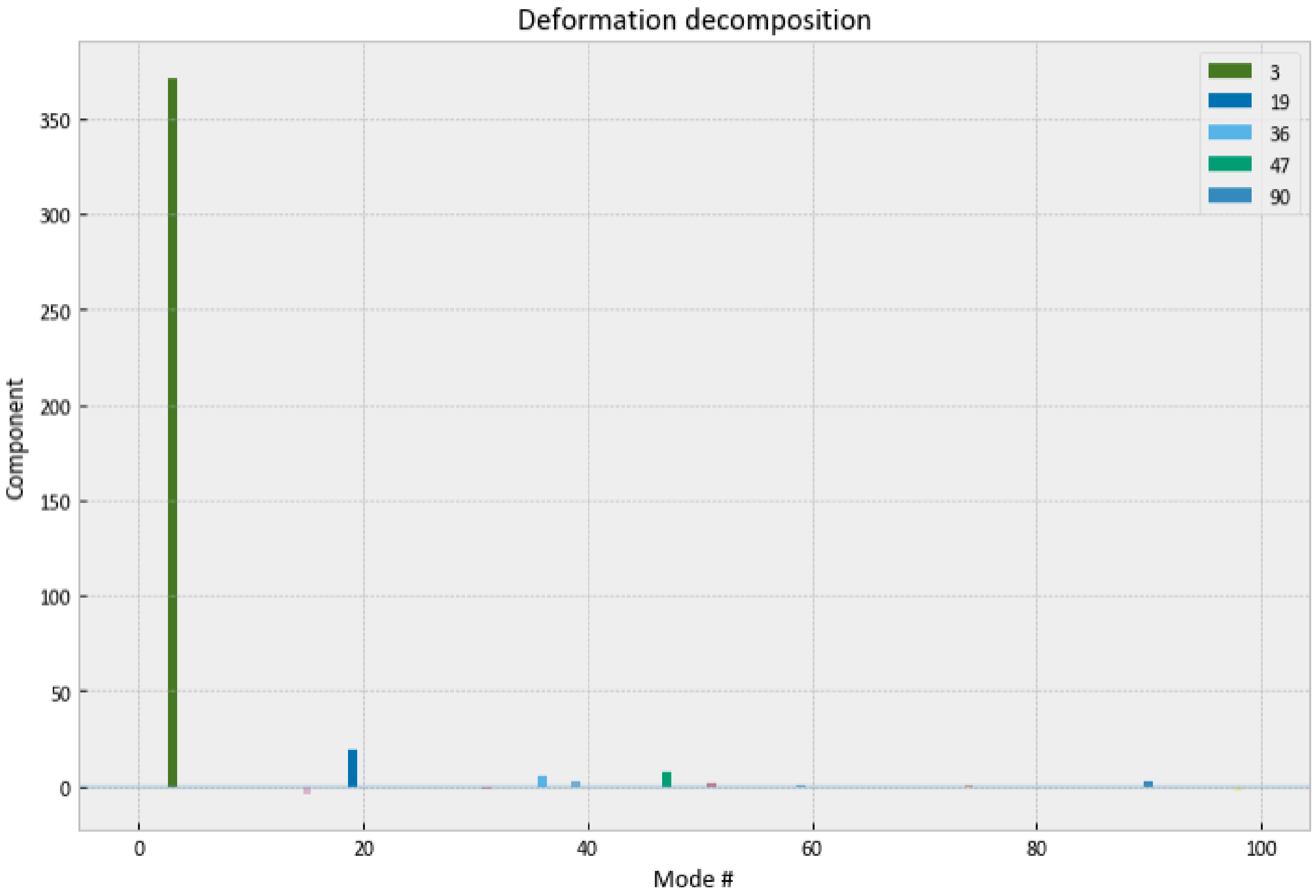

Target deformation decomposition in the static-problem eigenmodes.

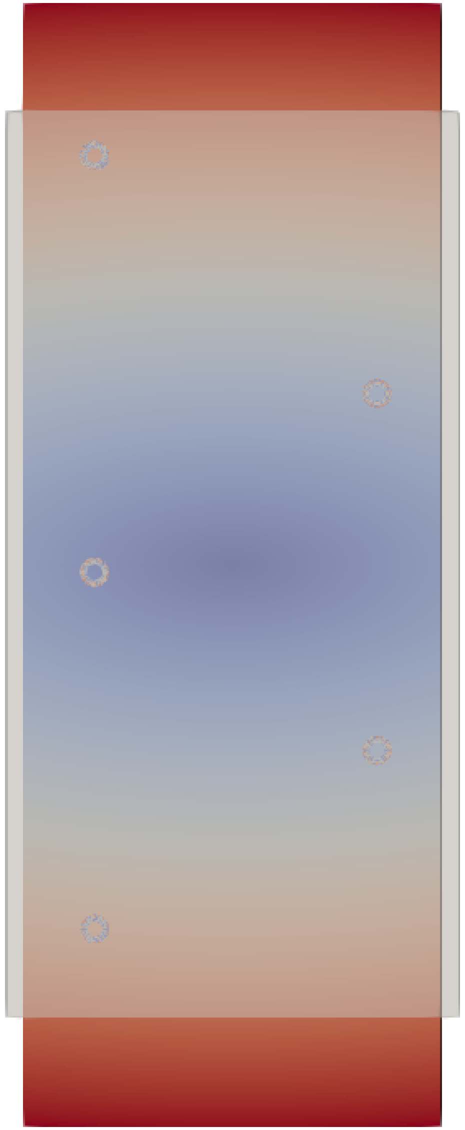

Transducers, natural state and target deformed state.
(300x deformation scale)

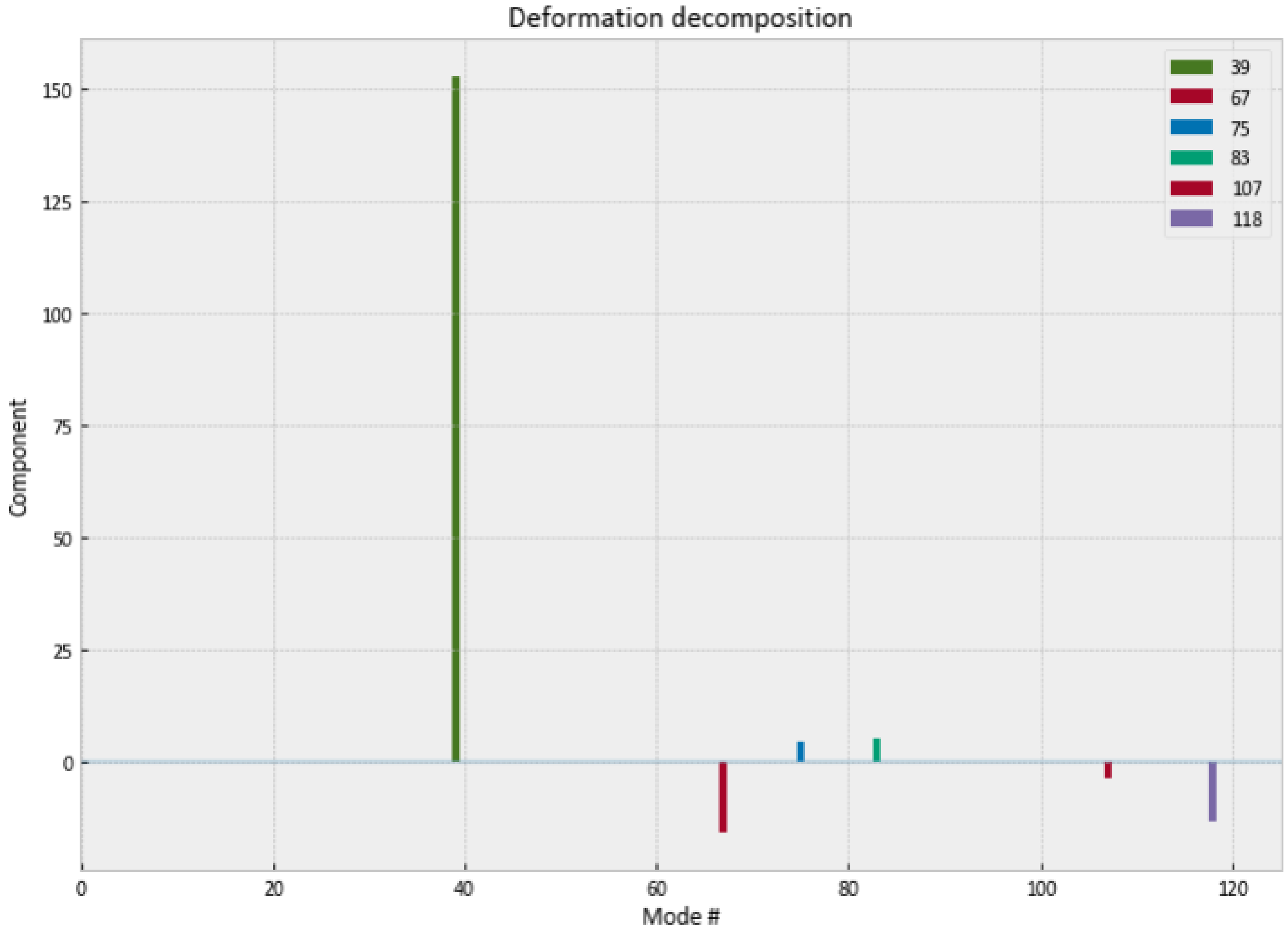

Target deformation decomposition in the static-problem eigenmodes.

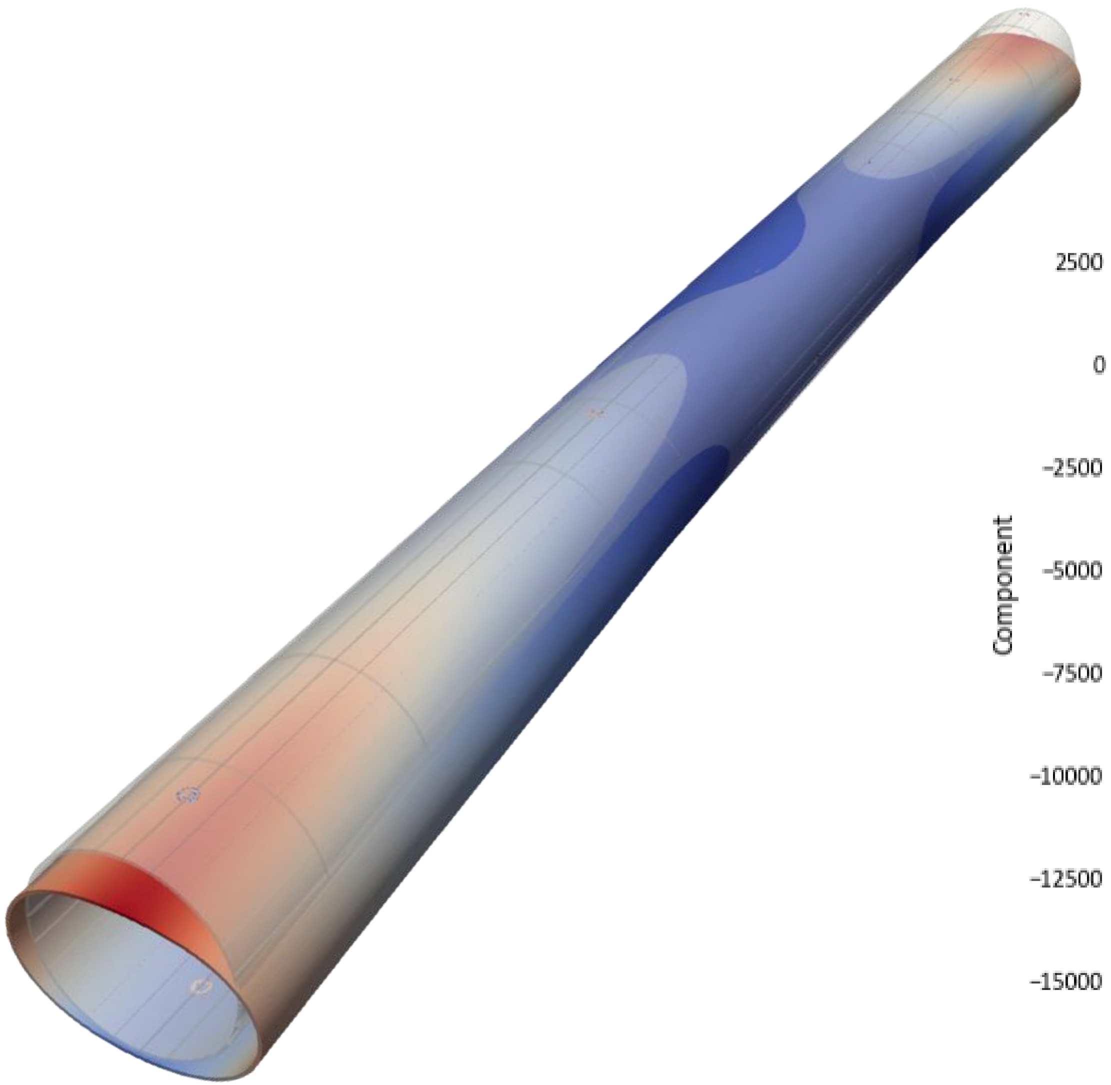

Transducers, natural state and target deformed state.
(3x deformation scale)

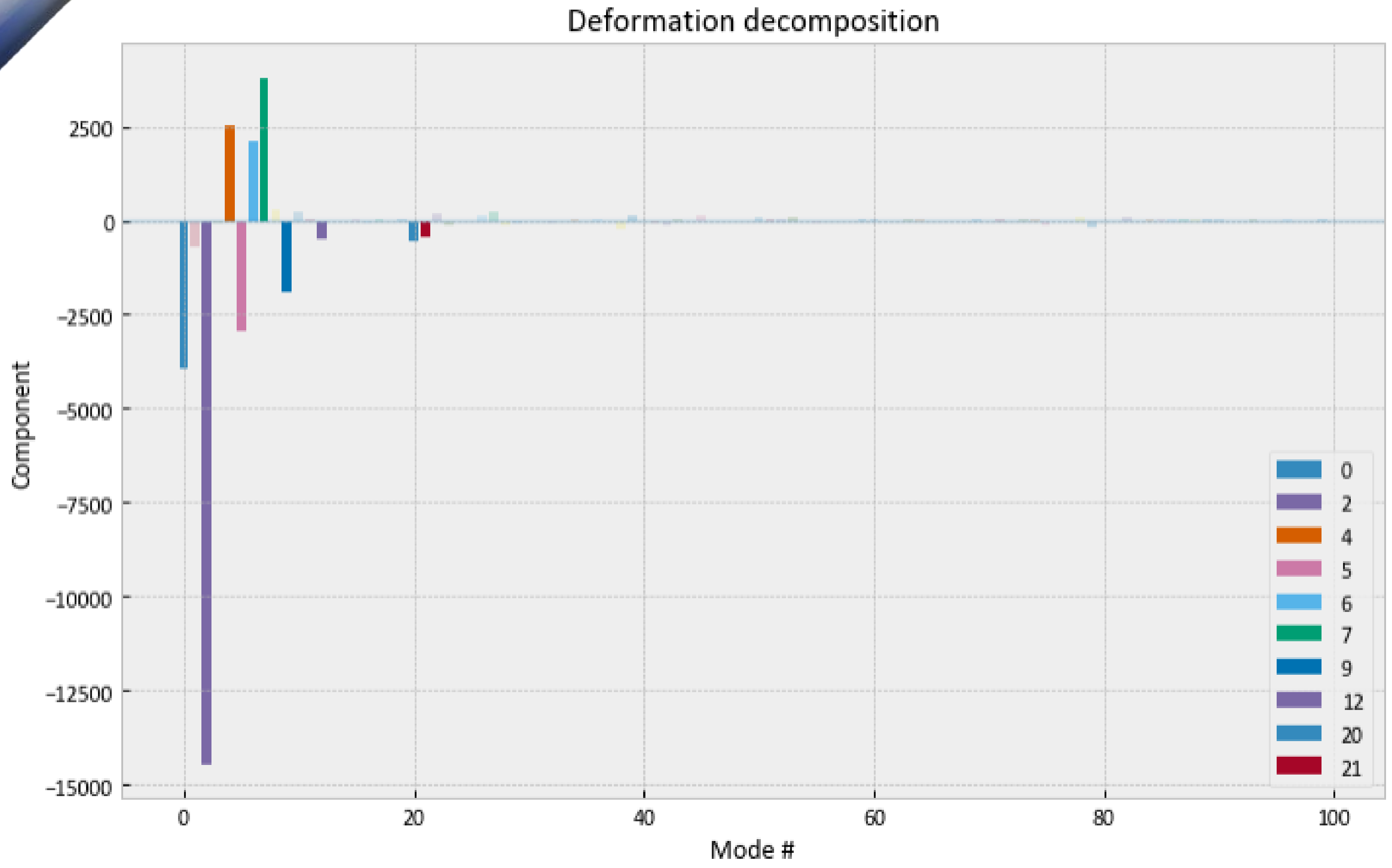

Target deformation decomposition in the static-problem eigenmodes.

Objective: Estimate without the *a priori*.

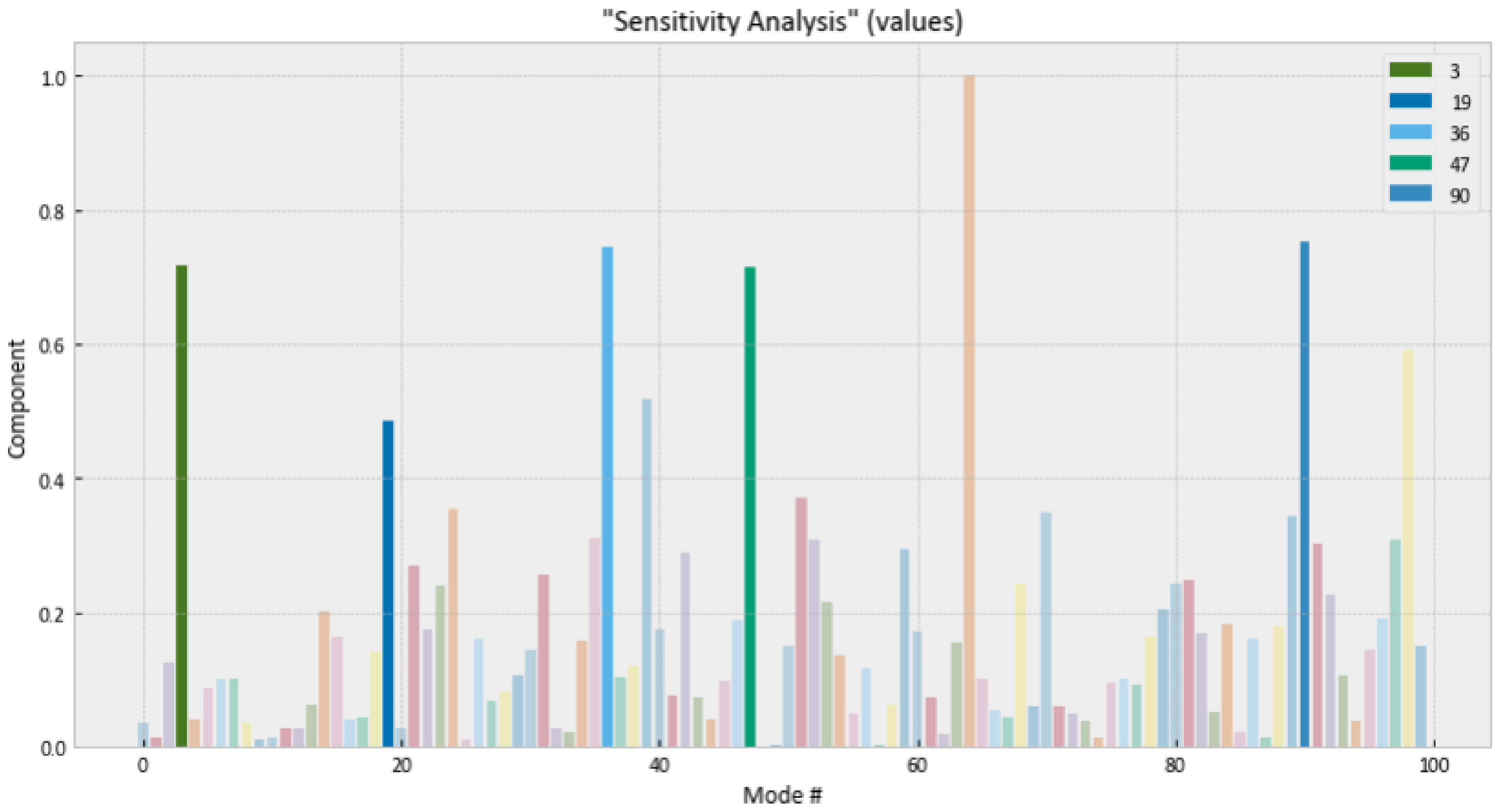

Objective: Estimate without the *a priori*.